SANDIA REPORT

SAND96–1197 • UC–403
Unlimited Release
Printed May 1996

Gas-Phase Diffusion in Porous Media - Evaluation of an Advective-Dispersive Formulation and the Dusty-Gas Model Including Comparison to Data for Binary Mixtures

Stephen W. Webb

Prepared by
Sandia National Laboratories
Albuquerque, New Mexico 87185 and Livermore, California 94550
for the United States Department of Energy
under Contract DE-AC04-94AL85000

Issued by Sandia National Laboratories, operated for the United States Department of Energy by Sandia Corporation.

Available to DOE and DOE contractors from
Office of Scientific and Technical Information
PO Box 62
Oak Ridge, TN 37831

Prices available from (615) 576-8401, FTS 626-8401

Available to the public from
National Technical Information Service
US Department of Commerce
5285 Port Royal Rd
Springfield, VA 22161

NTIS price codes
Printed copy: A04
Microfiche copy: A01

SAND96-1197
Unlimited Release
Printed May 1996

Distribution
Category UC-403

Gas-Phase Diffusion in Porous Media - Evaluation of an Advective-Dispersive Formulation and the Dusty-Gas Model Including Comparison to Data for Binary Mixtures

Stephen W. Webb
Geohydrology Department
Sandia National Laboratories
Albuquerque, NM 87185

ABSTRACT

Two models for gas-phase diffusion and advection in porous media, the Advective-Dispersive Model (ADM) and the Dusty-Gas Model (DGM), are reviewed. The ADM, which is more widely used, is based on a linear addition of advection calculated by Darcy's Law and ordinary diffusion using Fick's Law. Knudsen diffusion is often included through the use of a Klinkenberg factor for advection, while the effect of a porous medium on the diffusion process is through a porosity-tortuosity-gas saturation multiplier. Another, more comprehensive approach for gas-phase transport in porous media has been formulated by Evans and Mason, and is referred to as the Dusty-Gas Model (DGM). This model applies the kinetic theory of gases to the gaseous components and the porous media (or "dust") to develop an approach for combined transport due to ordinary and Knudsen diffusion and advection including porous medium effects.

While these two models both consider advection and diffusion, the formulations are considerably different, especially for ordinary diffusion. The various components of flow (advection and diffusion) are compared for both models. Results from these two models are compared to isothermal experimental data for He-Ar gas diffusion in a low-permeability graphite. Air-water vapor comparisons have also been performed, although data are not available, for the low-permeability graphite system used for the helium - argon data. Radial and linear air-water heat pipes involving heat, advection, capillary transport, and diffusion under nonisothermal conditions have also been considered.

Based on the data-model comparisons, the DGM is recommended for gas-phase transport analyses in porous media. As discussed in the derivation of the DGM, Fick's Law must be defined relative to the mole-average velocity to calculate gas diffusion in porous media; the stationary coordinate definition used in the advective-dispersive formulation discussed here is inappropriate and may lead to significant errors in the component fluxes, especially for stagnant conditions. Additional data-model comparisons are needed for air-VOC systems, multicomponent mixtures, and actual soils including unsaturated conditions.

Table of Contents

List of Figures

List of Tables

1.0 INTRODUCTION

Gas-phase diffusion in porous media may be significant in the flow of multiphase fluids and the transport of contaminants in the subsurface. In many applications, such as removal of nonaqueous phase liquid (NAPL) contaminants from low-permeability layers in the subsurface, gas-phase diffusion may be the limiting transport mechanism. Gas-phase diffusion may also be important in the analysis of contaminant migration and/or drying processes in potential nuclear waste repositories such as Yucca Mountain (Pruess and Tsang, 1993; Finsterle, Schlueter, and Pruess, 1990; Tsang and Pruess, 1990), and in porous catalysts (Jackson, 1977).

A number of different models for combined advection-diffusion of gases in porous media have been employed. The most widely used model is the Advective-Dispersive Model, or ADM, which is based on a linear addition of advection calculated by Darcy's Law and ordinary diffusion using Fick's Law. Knudsen diffusion is often included through the use of a Klinkenberg factor for advection, while the effect of a porous medium on the diffusion process is through a porosity-tortuosity-gas saturation multiplier. This model is employed in TOUGH2 (Pruess, 1991), a widely-used code for simulating flow and transport in fractured and porous media in nuclear waste, environmental, and geothermal applications (Pruess, 1995), the PNL code STOMP (Lenhard et al., 1995), and has been proposed as the model for the new Sandia massively parallel porous media code (Martinez, 1995a,b). Another, more comprehensive approach for gas-phase transport in porous media has been formulated by Evans and Mason in a series of papers between 1961 and 1967, which is referred to as the Dusty-Gas Model (DGM). This model applies the kinetic theory of gases to the gaseous components and the porous media (or "dust") to develop an approach for combined transport due to ordinary and Knudsen diffusion and advection including porous medium effects.

While these two models both consider advection and diffusion, the formulations are considerably different, especially for diffusion. A comparison of the predictions from these two approaches including available experimental data has been performed to illustrate the differences between the two models. Experimental data used include combined advection and diffusion of binary gas mixtures in a low-permeability porous medium.

A review of these two gas-phase diffusion models for porous media is given in the next section, followed by comparison of the two models to gas-phase diffusion data restricted to a binary system. Application of the various models to more than two components is treated in references cited in the model descriptions.

The present research has been performed as part of Sandia Laboratory Directed Research and Development (LDRD) Project (Proposal 96-0236) entitled "Enhanced Vapor-Phase Diffusion in Porous Media."

2.0 REVIEW OF MODELS

The Advective-Dispersive Model (ADM) and the Dusty-Gas Model (DGM) are reviewed in this section.

2.1 Advective-Dispersive Model

The most common model for gas diffusion and advection in porous media is the Advective-Dispersive Model (ADM). This approach is employed in TOUGH2 (Pruess, 1991), a widely-used code for simulating flow and transport in fractured and porous media in nuclear waste, environmental, and geothermal applications, the PNL code STOMP (Lenhard et al., 1995), and has been proposed as the model for the new Sandia massively parallel porous media code (Martinez, 1995a,b). A number of other investigators, including Abriola and Pinder (1985), have used a similar approach. Note that the ADM is also used in T2VOC (Falta et al., 1995) and M^2NOTS (Adenekan et al., 1993) for multicomponent diffusion transport of NAPLs (nonaqueous phase liquids) and VOCs (volatile organic compounds) along with water vapor and air because both of these codes are based on TOUGH2.

The ADM is based on a linear addition of advection calculated by Darcy's Law and ordinary diffusion using Fick's Law. Slip effects, or Knudsen diffusion, are included through a Klinkenberg parameter to define the effective permeability for the advective mass flux. Porous medium effects for ordinary diffusion are included through a porosity-tortuosity-gas saturation factor on the diffusive mass flux in free space.

In the discussion that follows, gas-phase only conditions (S_g=1.0) will be assumed because the primary emphasis of the present study is gas-phase transport. Unsaturated conditions with simultaneous gas-phase and liquid-phase flow will be discussed in the heat pipe simulations presented in the Model Comparisons section of this report.

As given by Pruess (1987, 1991), the ADM mass flux for component i, F_i, for the gas-phase only case is

$$F_i = -\frac{k}{\mu}\rho_g \omega_i(\nabla P_g - \rho_g g_c) - D_{12}\rho_g \nabla\omega_i \qquad (1)$$

where k is the permeability, μ is the viscosity, P_g is the gas pressure, ω is the mass fraction, ρ is the density, g_c is the gravitational constant, and D_{12} is the effective diffusion coefficient. The first term on the right hand side is the advective mass flux and the second term is the diffusive mass flux.

Slip, or Knudsen diffusion, is simply incorporated into the model through modification of the permeability by the Klinkenberg factor, b, as

$$k = k_0(1 + b/P_g) \tag{2}$$

where k_0 is the intrinsic permeability and P_g is the gas pressure.

The effective diffusion coefficient is a function of pressure and temperature and porous media parameters, or

$$D_{12} = \tau\phi S_g D_{12}^0 \frac{P_0}{P}\left(\frac{T+273.15}{273.15}\right)^\theta \tag{3}$$

where τ is the tortuosity, ϕ is the porosity, S_g is the gas saturation, D_{12}^0 is the binary diffusion coefficient at 1 bar (10^5 Pa) and 0° C in free space, P_0 is equal to 1 bar, T is the temperature in °C, and the exponent θ is typically 1.8 (Pruess, 1987).

In the case of pure ordinary diffusion (no advection), the ADM reduces to

$$F_{i=1} = - D_{12}\rho_g \nabla\omega_{i=1} \tag{4}$$

$$F_{i=2} = - D_{21}\rho_g \nabla\omega_{i=2} \, . \tag{5}$$

For a binary mixture, $\nabla\omega_{i=1} = - \nabla\omega_{i=2}$, and $D_{12} = D_{21}$, so

$$F_{i=1} = F_{i=2} \, , \tag{6}$$

and the mass fluxes of the two components are equal and opposite.

2.2 Dusty-Gas Model

The Dusty-Gas Model (DGM) was developed to describe gas transport through porous media including the coupling between the various transport mechanisms. The term dusty-gas is used because the porous medium is a component of the gas mixture consisting of large molecules fixed in space, and the kinetic theory of gases is applied to this dusty-gas mixture. The DGM is discussed in detail by Mason and Malinauskas (1983) and by Cunningham and Williams (1980).

Hadley (1982) developed a model which, according to the author, is "essentially identical" to the model of Mason, Malinauskas, and Evans (1967), or the DGM. The numerical simulators PETROS (Hadley, 1985) and NORIA (Bixler, 1985) are based on the Hadley model. PETROS and NORIA have had limited use and are planned to be replaced by the simulator being developed by Martinez (1995a,b) which is currently based on an advection-dispersion model similar to TOUGH2.

Gas transport through porous media can be divided into three independent modes:

(1) Free-molecule or Knudsen diffusion, which is dominated by molecule-wall collisions;
(2) Advective flow, which is dominated by molecule-molecule collisions;
(3) Continuum or ordinary diffusion due to concentration gradients, temperature gradients, or external forces, which is dominated by molecule-molecule collisions.

For simplicity, the discussion below is limited to a binary gas, and temperature gradients and external forces such as gravity are ignored. The more complex nonisothermal and/or multicomponent system is treated in the DGM references given above.

One of the key ingredients in the DGM is combination of the correct form of the various mechanisms for diffusion (ordinary and Knudsen) and advection. Ordinary and Knudsen diffusion are combined through additivity of momentum transfer based on kinetic-theory arguments, and diffusive (ordinary plus Knudsen) fluxes are added to advective fluxes based on Chapman-Enskog kinetic theory. In order for these fluxes to be additive, there must be no coupling or interaction between them. In other words, the definition of diffusion must not cause viscous flow, and viscous flow must not cause diffusive flow. This coupling will be discussed in more detail below when the form of ordinary diffusion is discussed.

The presentation that follows is essentially from Mason and Malinauskas (1983). Mason and colleagues (Evans, Watson, and Mason, 1961, 1962; Mason et al., 1963, 1964, 1967) developed the theory over a number of years using a full Chapman-Enskog kinetic-theory treatment for the gas mixture in which the porous medium is considered to be the "dust" in the gas. The treatment below is based on simpler momentum transfer arguments, which give the same results.

2.2.1 Gas Transport Mechanisms

2.2.1.1 Knudsen Diffusion

Knudsen diffusion, which is operative in the free-molecule region, is dependent on the gradient of the gas density of each species independent of each other. In the free-molecule regime, the molecular mean free path is larger than the characteristic dimension of the medium, so molecule-wall interactions dominate over molecule-molecule interactions. The net flux of species i in Knudsen diffusion is proportional to the gradient of the molecular density, n, or

$$J_{iK} = - D_{iK} \nabla n_i \tag{7}$$

where

$$D_{iK} = (4/3)\ K_o v_i \tag{8}$$

and v is the mean molecular speed

$$v = (8 k_B T/\pi m)^{1/2} \tag{9}$$

and k_B is Boltzmann's constant, T is the temperature, and m is the molecular mass. The parameter K_o is dependent on the scattering medium or the porous medium and is usually measured. Note that D_{iK} is independent of pressure and is proportional to $T^{1/2}$.

Consider a thin plate in open space with a small hole in it. Two different gases are on either side of the plate at the same pressure and temperature. The value of K_o is the same for both gases. Due to Knudsen diffusion, gas will diffuse from one side to the other, and the ratio of the fluxes is

$$-J_{1K}/J_{2K} = D_{1K}/D_{2K} = v_1/v_2 = (m_2/m_1)^{1/2}\ . \tag{10}$$

This relationship is known as Graham's law of effusion and was discovered in 1846 (Graham, 1846).

The diffusive flux due to Knudsen diffusion is similar to ordinary diffusion in that the diffusive flux is due to a molecular density gradient. The difference between the two types of diffusion is due to the dominant type of molecular collisions of each process. Knudsen diffusion is in the free-molecular region with minimal molecule-molecule collisions; molecule-wall collisions dominate. Ordinary diffusion is dominated by molecule-molecule collisions. Therefore, each diffusion mechanism has its own dominant molecular collision process and its own diffusion coefficient.

2.2.1.2 Advective Flow

Advective flow is straightforward. The flow rate in a porous medium is linearly dependent on the pressure gradient, the permeability, the molecular density, and inversely proportional to the fluid viscosity, or

$$J_{adv} = -(nk/\mu)\nabla P_g \ . \tag{11}$$

The flux is directly proportional to pressure through the molecular density term. All species in a mixture are transported at the same rate by advective flow, so the flux of any species is simply

$$J_{i,adv} = x_i J_{adv} \tag{12}$$

and advective flow does not lead to separation of the different species being transported.

2.2.1.3 Ordinary Diffusion

Ordinary diffusion is the most difficult of the three transport mechanisms to properly define. While the ADM assumes direct applicability of Fick's Law, there are subtle complications when advection is involved as discussed below.

Suppose we have two gases in two bulbs connected by a tube as indicated in Figure 1. Each bulb is at the same temperature and pressure, and no external forces exist. Assume that the piston in the figure is fixed, so the volume of each bulb is constant. In this situation, the lighter (and faster) molecules diffuse more quickly than the heavier (and slower) molecules due to their higher speed, so the net diffusive molar flux will be towards the bulb with the heavy gas. This diffusive flux will cause an increase in the pressure in the heavy gas bulb (and a decrease in the pressure in the lighter gas bulb), resulting in viscous flow from the heavier gas bulb to the lighter gas bulb in the opposite direction of diffusion. This change in pressure, and resulting advective flow, violates the independence of the two mechanisms as outlined above.

Now suppose we have the same scenario as discussed above but we allow the piston to move to maintain equal pressures. Again, the lighter gas will diffuse faster than the heavier gas, and there will be a net flow of gas between the two bulbs. The piston will move to the left to keep the pressures constant. In order to have a zero pressure gradient and zero advective flux due to diffusion and to maintain the simple additivity of the viscous and diffusive fluxes, diffusion must be defined in a coordinate system moving with the average molar velocity.

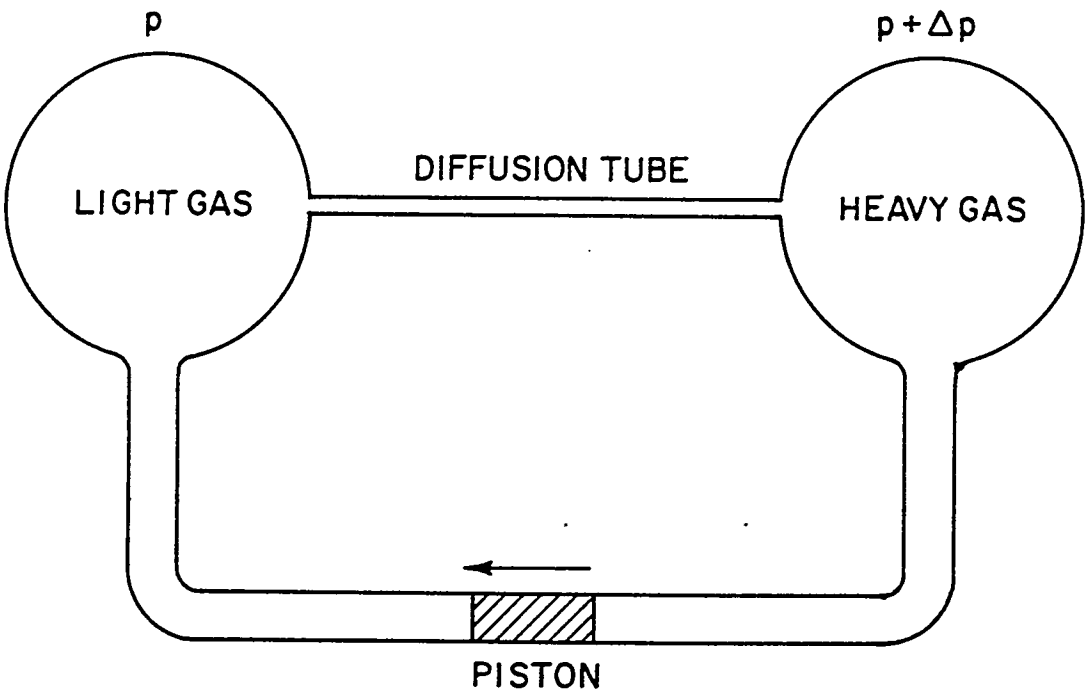

Figure 1
Binary diffusion. If the piston is held stationary, a pressure difference develops that is just sufficient to keep the net flux zero through the diffusion tube. If the pressure is kept uniform, the piston must be moved as indicated, and there is a net flux of gas through the diffusion tube. (figure and caption from Mason and Malinauskas, 1983)

As discussed by Mason and Malinauskas (1983) and by Bird, Stewart and Lightfoot (1960) for a binary mixture, the molar diffusive flux of components 1 and 2 relative to stationary coordinates is

$$J_{1D} = - D_{12} \nabla n_1 + x_1 J_D \tag{13}$$

$$J_{2D} = - D_{21} \nabla n_2 + x_2 J_D \tag{14}$$

where D_{12} is the effective binary diffusion coefficient and $J_D = J_{1D} + J_{2D}$ is the net molar flux and $x_i = n_i/n$ is the mole fraction. Diffusion is defined relative to the molar average velocity, J_D/n.

For equal pressure diffusion, such as when the piston moves, the ratio of the diffusive fluxes is given by

$$-J_{1D}/J_{2D} = (m_2/m_1)^{1/2} \tag{15}$$

which was experimentally discovered by Graham (1833). While this ratio is the same as Graham's law of effusion, it is quite different in applicability and is called Graham's law of diffusion. This relationship is not applicable if there is any pressure difference.

A simple derivation of this relationship can be performed by considering momentum transferred to the walls by molecular collisions as given by Mason and Malinauskas (1983). The net momentum transferred to the walls is the sum from the two diffusive fluxes. This sum must equal zero if there is no pressure gradient, or

$$J_{1D} m_1 v_1 + J_{2D} m_2 v_2 = 0 \ , \tag{16}$$

or

$$- J_{1D}/J_{2D} = m_2 v_2/m_1 v_1 = (m_2/m_1)^{1/2} \tag{17}$$

where use has been made of the molecular speed relationship given earlier.

As mentioned above, this ratio was discovered experimentally by Graham in 1833. Unfortunately, the requirement of equal pressures was overlooked, and the above relationship was assumed to be simply an approximation and was forgotten until Hoogschagen

rediscovered it (Hoogschagen, 1953, 1955). The problem was that most diffusion experiments were carried out in a closed two-bulb system with a small, but not negligible, pressure difference. In interpretation of these experiments, the pressure difference set up a viscous flux that was not considered in interpretation of the data; only transport by diffusion was considered.

2.2.2 Combined Transport

Knudsen diffusion and ordinary, or continuum diffusion, can be combined by consideration of momentum forces. If no external forces, such as gravity, are present, the momentum transferred to the walls must be balanced by some force. In the case of diffusion, this force is attributed to the partial pressure of each species. The Knudsen and ordinary diffusion flux equations (7 and 13) can be written as

$$-(\nabla P_{g,1})_{wall} = (k_B T / D_{1K})\, J_{1K} \,, \tag{18}$$

$$-(\nabla P_{g,1})_{molecule} = (k_B T / D_{12})\, (J_{1D} - x_1 J_D) \,, \tag{19}$$

where $P_{g,1} = n_1 k_B T$. These two pressure drop or momentum components are additive, so

$$-(\nabla P_{g,1}) = (k_B T / D_{1K})\, J_{1K} + (k_B T / D_{12})\, (J_{1D} - x_1 J_D) \,, \tag{20}$$

and a similar equation for the other species. This equation describes the diffusion for one component of a binary mixture with uniform total pressure including Knudsen and ordinary diffusion.

Note that in the ADM, the effect of Knudsen diffusion is only included in the effective permeability of the porous medium, which does not lead to separation of the components of the binary gas. Inclusion of Knudsen diffusion in the diffusive term in the DGM with the resulting separation of the components is one of the main differences in behavior between the ADM and the DGM.

If the pressure gradient is not zero, advection also occurs. Advection is simply added to the diffusive (Knudsen plus ordinary) flux since there are no direct coupling terms as long as diffusion is properly defined and does not implicitly include viscous flux contributions. For the DGM, the total flux is simply the sum of the various fluxes, or

$$J_1 = J_{1D} + J_{1,adv} = J_{1D} + x_1 J_{adv} \,, \tag{21}$$

$$J_2 = J_{2D} + J_{2,adv} = J_{2D} + x_2 J_{adv} \,, \tag{22}$$

$$J = J_1 + J_2 = J_D + J_{adv} \,. \tag{23}$$

As shown by Mason and Malinauskas (1983), the various expressions for the individual fluxes can be combined resulting in

$$J_1 = - D_1 \nabla n_1 + x_1 \delta_1 J - x_1 \gamma_1 \left(\frac{nk}{\mu}\right) \nabla P_g \,, \tag{24}$$

$$J_2 = - D_2 \nabla n_2 + x_2 \delta_2 J - x_2 \gamma_2 \left(\frac{nk}{\mu}\right) \nabla P_g \,, \tag{25}$$

where

$$\frac{1}{D_1} = \frac{1}{D_{1K}} + \frac{1}{D_{12}} \tag{26}$$

$$\delta_1 = \frac{D_1}{D_{12}} = \frac{D_{1K}}{D_{1K} + D_{12}} \tag{27}$$

$$\gamma_1 = \frac{D_1}{D_{1K}} = \frac{D_{12}}{D_{1K} + D_{12}} = 1 - \delta_1 \,. \tag{28}$$

Multicomponent versions of the above equations are given by Mason and Malinauskas (1983).

There are many alternative forms of the DGM which can be derived by combining various forms of the equations. Thorstenson and Pollock (1989) present a number of useful forms, including specific forms for binary systems which is of special interest here. In particular, using the above equations and some patience, the total flux of component 1 in an isothermal binary system can be written as

$$J_1 = - \frac{\left[D_{1K} D_{12} \frac{P_g}{RT} \nabla x_1 + D_{1K} (D_{12} + D_{2K}) x_1 \frac{\nabla P_g}{RT} \right]}{(D_{12} + x_1 D_{2K} + x_2 D_{1K})} - x_1 \frac{k P_g}{\mu} \frac{\nabla P_g}{RT} \quad (29)$$

and

$$J = J_1 + J_2 = \frac{\left[D_{12} (D_{2K} - D_{1K}) \frac{P_g}{RT} \nabla x_1 - \left(D_{12} (x_1 D_{1K} + x_2 D_{2K}) + D_{1K} D_{2K} \right) \frac{\nabla P_g}{RT} \right]}{(D_{12} + x_1 D_{2K} + x_2 D_{1K})} - \frac{k P_g}{\mu} \frac{\nabla P_g}{RT} \quad (30)$$

Thorstenson and Pollock (1989) also present other forms of the above total flux equation including limiting forms of the equation for different regimes, such as the Knudsen regime and the ordinary (molecular) diffusion regime.

Two items are of particular interest. First, the diffusion flux in the component equation is dependent on both Knudsen diffusion and ordinary diffusion coefficients. The reason is that Knudsen diffusion characterizes the wall-molecule interaction of diffusion, while Fick's Law only considers molecule-molecule processes. Second, the first term in the total flux equation is dependent on the difference in the Knudsen diffusion coefficients of the two gas components. Therefore, the coefficient is not a single value but is dependent on the specific gases involved as shown by Klinkenberg (1941). The above equations are of the same form as ADM; the two forms are compared in the section 2.4.

The above equations and derivations are for an isothermal system. If a temperature gradient also exists, such as in a heat pipe, thermal transpiration and thermal diffusion also occur due to the temperature gradient. However, as discussed by Mason and Malinauskas (1983), while thermal transpiration and thermal diffusion may not be negligible, they are not dominant either, based on the analyses of Wong et al. (1975, 1976) who employed the DGM. Predictive models for the thermal transpiration and thermal diffusion coefficients, where available, are complicated at the present time, and their accuracy is only moderate. Therefore, thermal transpiration and thermal diffusion are not included in the present study.

2.3 Comparison of Model Requirements

The ADM and DGM models are significantly different from each other as can be seen by comparing the appropriate equations (equations 1 and 2 for ADM and equation 29 for DGM) and as discussed in more detail in the next section. In spite of these dramatically different formulations, the data requirements for the two approaches are the same. Both models need the permeability and an effective binary diffusion coefficient, which are identical in both

models. For Knudsen diffusion, the ADM relies on a Klinkenberg parameter. While the DGM uses two separate Knudsen diffusion coefficients, the ratio between the component values is simply dependent on the ratio of molecular weights, and the Klinkenberg parameter can be used directly to calculate the Knudsen diffusion coefficients. Therefore, there are no differences in the data requirements between the two models.

2.4 ADM - DGM Comparison

The ADM and DGM are compared in this section. Farr (1990) did some similar, although more limited, comparisons along the same lines. In the present comparison, the ratio of the various mass fluxes for advective flow, Knudsen diffusion, and ordinary diffusion neglecting the gravitational term for simplicity will be evaluated.

ADM - Mass fluxes

Combining equations (1) and (2), the appropriate equation for the ADM is:

$$F_i = -\frac{k}{\mu}\rho_g \omega_i (1 + b/P_g)\nabla P_g - D_{12}\rho_g \nabla \omega_i \tag{31}$$

where the $(1+b/P_g)$ term includes the Klinkenberg factor, b, for Knudsen diffusion. This equation can be rearranged as follows

$$F_1 = -\left[\frac{k\rho_g \omega_1}{\mu}\frac{b}{P_g} + \frac{k\rho_g \omega_1}{\mu}\right]\nabla P_g - D_{12}\rho_g \nabla \omega_1 \,. \tag{32}$$

DGM - Molar fluxes

The appropriate equation for the DGM is equation (29), or

$$J_1 = -\frac{\left[D_{1K}D_{12}\frac{P_g}{RT}\nabla x_1 + D_{1K}(D_{12} + D_{2K})x_1\frac{\nabla P_g}{RT}\right]}{(D_{12} + x_1 D_{2K} + x_2 D_{1K})} - x_1\frac{kP_g}{\mu}\frac{\nabla P_g}{RT} \tag{33}$$

which can be rearranged as follows

$$J_1 = - \frac{D_{1K} D_{12} \frac{P_g}{RT}}{D^*} \nabla x_1 - \left[\frac{D_{1K}(D_{12} + D_{2K}) x_1 / RT}{D^*} + x_1 \frac{k P_g}{\mu RT} \right] \nabla P_g \quad (34)$$

where

$$D^* = D_{12} + x_1 D_{2K} + x_2 D_{1K} . \quad (35)$$

In each of these equations, the first term is ordinary diffusion, the second term is Knudsen diffusion, and the third term is advective flow. The ratios from the two formulations will be compared individually.

2.4.1 Advective Flow

ADM

$$F_{1\,adv}^{ADM} = - \frac{k \rho_g \omega_1}{\mu} \nabla P_g \quad (36)$$

In the present analysis of the ADM, the Klinkenberg factor, b, is not included in the advective flow contribution but is included in the Knudsen diffusion term.

DGM

$$F_{1\,adv}^{DGM} = J_{1\,adv}^{DGM} m_1 = - x_1 \frac{k}{\mu} \frac{P_g}{RT} m_1 \nabla P_g \quad (37)$$

In the DGM expression, P_g/RT is the molar density, so $x_1 P_g/RT$ is the molar density of phase 1. When this molar density of phase 1 is multiplied by the molecular weight, it results in the mass density of phase 1, or

$$x_1 \frac{P_g}{RT} m_1 = \rho_g \omega_1 . \quad (38)$$

Therefore, as expected, the advective fluxes from both models are equivalent, or

$$F_{1\ adv}^{DGM} = F_{1\ adv}^{ADM} \tag{39}$$

2.4.2 Knudsen Diffusion

ADM

$$F_{1\ Knudsen}^{ADM} = -\frac{k\rho_g\omega_1}{\mu}\frac{b}{P_g}\nabla P_g \tag{40}$$

DGM

$$F_{1\ Knudsen}^{DGM} = J_{1\ Knudsen}^{DGM} m_1 = -\left[\frac{D_{1K}(D_{12} + D_{2K})x_1/RT}{D^*}\right] m_1 \nabla P_g \tag{41}$$

Using the mole fraction - mass fraction relationship discussed above

$$x_1\frac{P_g}{RT}m_1 = \rho_g\omega_1\ , \tag{42}$$

the ratio of the mass fluxes can be written as

$$Ratio_{1\ Knudsen} = \frac{F_{1\ Knudsen}^{DGM}}{F_{1\ Knudsen}^{ADM}} = \frac{D_{1K}(D_{12} + D_{2K})/D^*}{kb/\mu} \tag{43}$$

and μ is the mixture viscosity. The Klinkenberg factor, b, is a single constant which is representative of the gas mixture. As shown by Klinkenberg (1941) and as discussed in detail by Thorstenson and Pollock (1989), b is a function of the gas and the porous medium. The Klinkenberg factor is proportional to $m^{-1/2}$, where m is the molecular weight. The Knudsen diffusivity used in the DGM is defined in terms of the Klinkenberg factor as shown in the Appendix as

$$D_{1K} = kb_1/\mu_1 \tag{44}$$

and the ratio is

$$Ratio_{1\ Knudsen} = \frac{b_1}{b}\frac{\mu}{\mu_1}\frac{(D_{12} + D_{2K})}{D_{12} + x_1 D_{2K} + x_2 D_{1K}} . \quad (45)$$

This ratio can vary from near unity for gases which have similar molecular weights and viscosities to large or small values when the molecular weights differ dramatically, such as for NAPLs and air.

In order to get an idea of the magnitude and variation of this ratio, several assumptions have been made. Assuming that the ADM model parameters are based on component 1 ($b = b_1$; $\mu = \mu_1$), that $D_{12} = D_{1K}$ (as will be seen later, the magnitude of the various diffusion coefficients are often similar), and using the Knudsen diffusion relationship

$$D_{jK} = D_{iK}\left(\frac{m_i}{m_j}\right)^{1/2} , \quad (46)$$

the ratio can be written as

$$Ratio_{1\ Knudsen} \approx \frac{1 + m_{rat}^{1/2}}{1 + x_2 + x_1 m_{rat}^{1/2}} \quad (47)$$

where

$$m_{rat} = \left(\frac{m_1}{m_2}\right) . \quad (48)$$

Again, note that equation (47) includes a number of assumptions. This ratio is shown in Figure 2 as a function of x_1 and the molecular weight ratio, m_{rat}, and is a strong function of these parameters. If the mole fraction x_1 is equal to 1.0, there is no difference between the two formulations. As the mole fraction of component 1 decreases, the ratio deviates from 1.0. For a molecular weight ratio of 10, the ratio increases from 1.0 to about 2.1 as x_1 goes to zero. For a large molecular weight ratio, the difference between the component Knudsen diffusion coefficients increases, leading to larger differences in the individual component fluxes. As x_1 decreases, component 2 plays a more significant role, and the differences are accentuated. For a molecular weight ratio of 1.6, which is the value for an air-water vapor mixture, the differences are significantly smaller, reaching a maximum of only about 1.2.

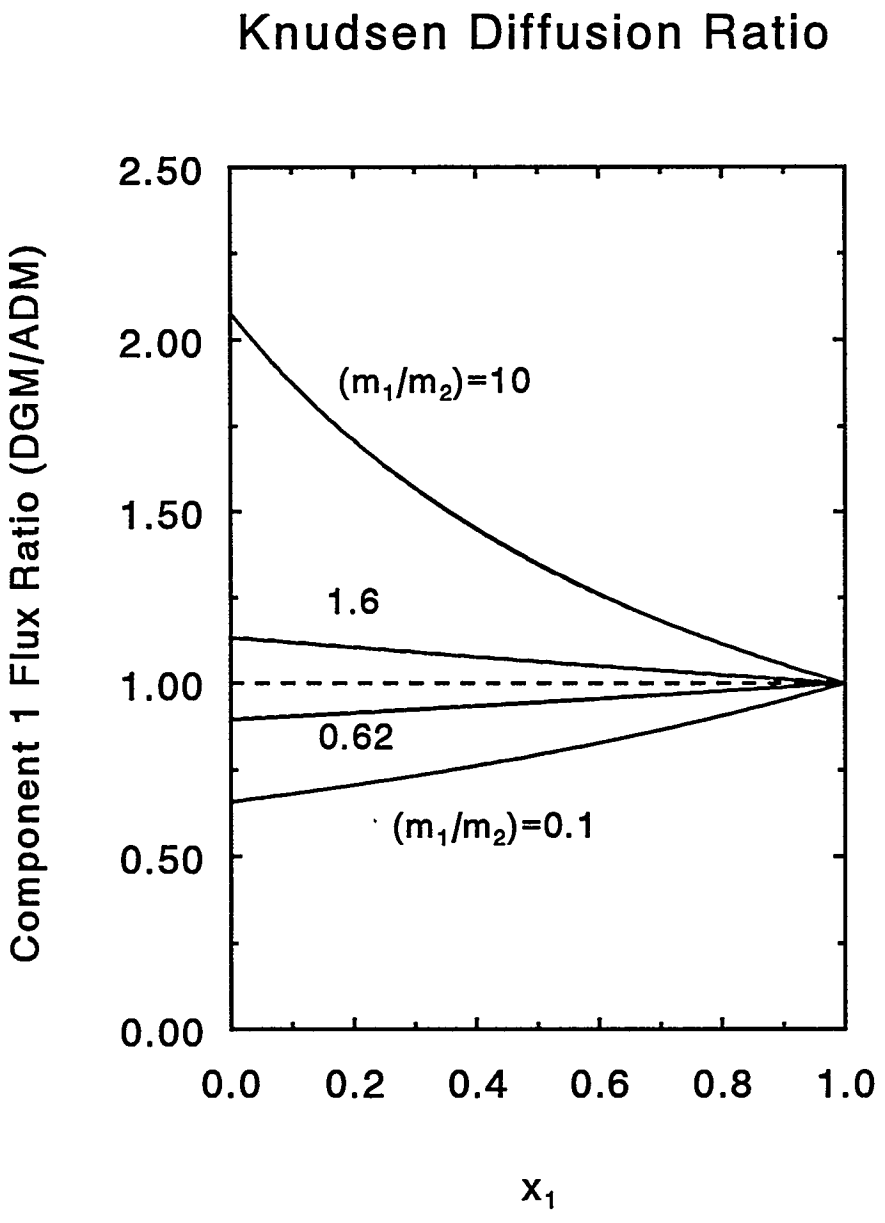

Figure 2
Comparison of ADM and DGM for Knudsen Diffusion

2.4.3 Ordinary Diffusion

ADM

$$F_{1\ diffusion}^{ADM} = - D_{12}\rho_g \nabla\omega_1 \tag{49}$$

DGM

$$F_{1\ diffusion}^{DGM} = J_{1\ diffusion}^{DGM}\ m_1 = -\frac{D_{1K}D_{12}\frac{P_g}{RT}}{D^*} m_1 \nabla x_1 \tag{50}$$

Using the mass fraction - mole fraction relationship discussed above, and the relationship from Bird, Stewart, and Lightfoot (1960) to go from a mole fraction gradient to a mass fraction gradient

$$\nabla\omega_1 = \frac{m_1 m_2 \nabla x_1}{(x_1 m_1 + x_2 m_2)^2} \tag{51}$$

the ratio between the two fluxes can be written as

$$Ratio_{1\ diffusion} = \frac{F_{1\ diffusion}^{DGM}}{F_{1\ diffusion}^{ADM}} = \frac{D_{1K}}{D^*}\frac{(x_1 m_1 + x_2 m_2)}{m_2} \tag{52}$$

Again, even in the case of ordinary diffusion, or diffusion due to a concentration gradient, the ratio depends on the Knudsen diffusion and ordinary diffusion coefficients.

Under the same assumption used in simplifying the Knudsen diffusion ratio of $D_{12}=D_{1K}$, the ratio can be expressed as

$$Ratio_{1\ diffusion} \approx \frac{x_2 + x_1 m_{rat}}{1 + x_2 + x_1 m_{rat}^{1/2}} \tag{53}$$

which is shown in Figure 3 as a function of the molecular weight ratio and x_1. Note that the ratio is always different from unity. Thus, under the current assumptions, there are practically no situations where the two formulations are the same. Even if the molecular weights are equal, the results will be different.

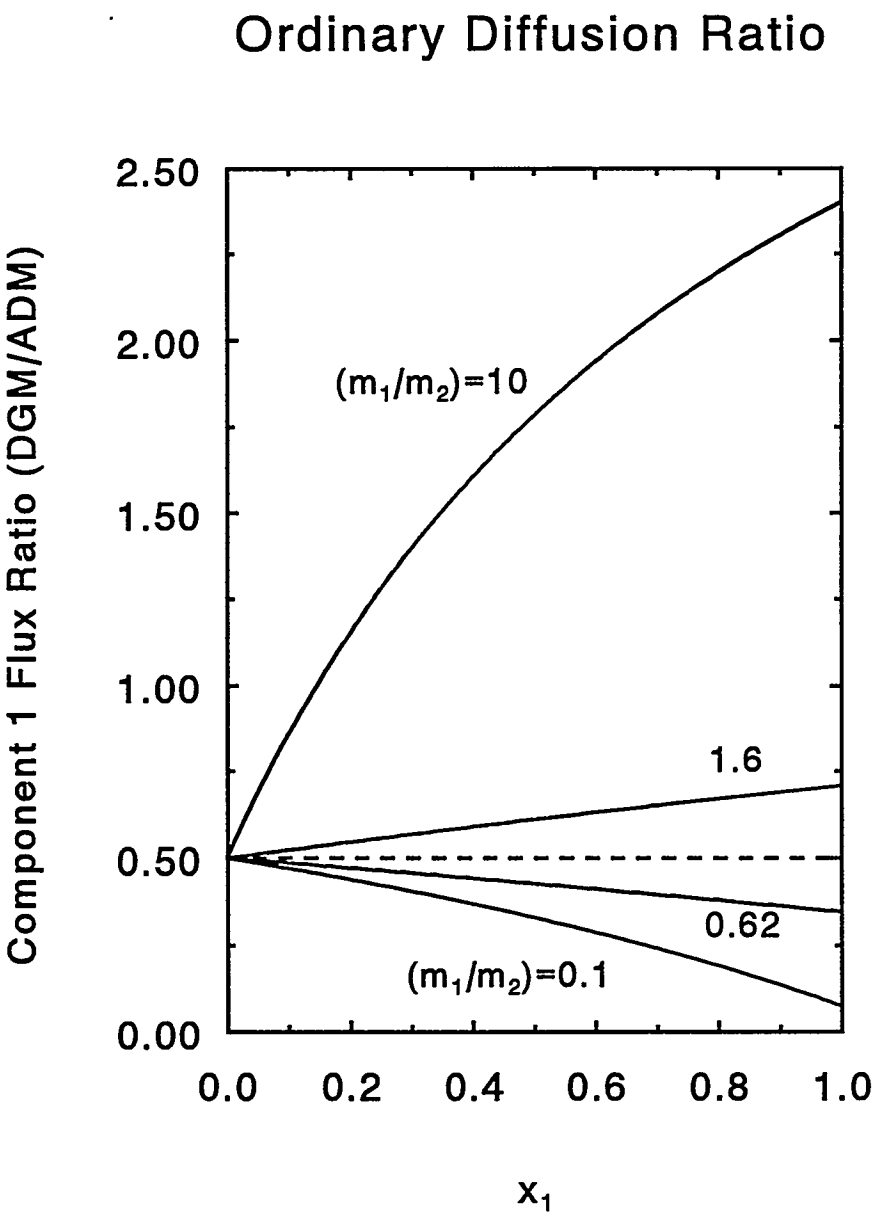

Figure 3
Comparison of ADM and DGM for Ordinary Diffusion

As was noted earlier, the two formulations have significantly different characteristics for ordinary diffusion. While the ADM results in equal and opposite mass fluxes, the DGM mole flux ratio is dependent on the molecular weight ratio, and ordinary diffusion is relative to the mole-average velocity, which is a function of the molecular weight ratio and the mole fractions. Therefore, the DGM/ADM ratio is a function of all the variables. The value of 0.5 at an x_1 value of 0. is due to the assumption of equal binary and Knudsen diffusion coefficients for component 1 and is simply equal to $D_{1K} / (D_{12} + D_{1K})$. Thus, for a higher permeability medium where Knudsen diffusion effects are small, the Knudsen diffusion coefficient is larger ($D_{iK} \propto k^{0.61}$ from the Appendix) implying smaller concentration gradients due to Knudsen diffusion. In this case, $D_{1K} \gg D_{12}$, and the ratio approaches 1.0 for x_1 equal to 0. As x_1 increases, the results from the two formulations will diverge unless the molecular weights are equal.

2.4.4 Overall Comparison

The ADM and DGM transport mechanisms have been compared above. While the advective flow formulations are identical, transport due to Knudsen diffusion and ordinary diffusion may be significantly different. The differences are a function of the molecular weights of the components, the mole fractions, and the ratio of ordinary and Knudsen diffusion coefficients.

The comparisons and ratios given in this section are only for individual mechanisms. Data-model comparisons are presented in the next section to compare the models under combined advection and diffusion conditions and to evaluate the performance of the two models compared to experimental data.

3.0 MODEL COMPARISONS

The predictions from the ADM and the DGM for pure diffusion and for combined advective flow and diffusion are presented in this section. The TOUGH2 code (Pruess, 1991), which uses the ADM in its original formulation, has been modified to use the DGM gas transport expressions. In the model comparisons that follow, only the transport expressions are different; the numerical scheme is the same for both models. In all cases, the computer times for the ADM and DGM models in TOUGH2 are essentially the same.

Note that Abriola et al. (1992) has previously compared an ADM with the DGM for transient transport of TCE and methane in soils. For advection-dominated cases such as for a high-permeability sandy soil (3×10^{-10} m^2), the difference between the two models is small. However, for a lower-permeability clay soil (1.25×10^{-16} m^2), the differences were significant. A similar effect has been alluded to in Section 2. No experimental data were included in their comparison.

The experimental data used for the present comparisons are from Evans, Watson, and Truitt (1962, 1963). They performed a number of experiments for flow and diffusion of helium and argon in a low-permeability graphite under various conditions in support of the DGM. The data include ordinary and Knudsen diffusion effects, and the fluxes of both gases were measured. These data were used to validate the DGM as given by Mason, Malinauskas, and Evans (1967) and as summarized by Mason and Malinauskas (1983) and by Cunningham and Williams (1980). The ADM and DGM predictions, including the TOUGH2 implementation of the DGM, will be compared to these data.

On a practical basis, many multiphase advection-diffusion problems involve air and water vapor. For this combination of gases (assuming air is a single component), the molecular weight ratio is only about 1.6 compared to approximately 10 for the helium-argon system studied by Evans, Watson, and Truitt. In addition, the mole differences for an air-water vapor system are considerably more limited for typical conditions due to water vapor condensation. The combination of a lower molecular weight ratio, which reduces the differences in diffusion between the two formulations, and the much lower mole fraction range invites further comparison for an air-water vapor system. Because experimental data on this combination are not available, predictions were performed for conditions similar to the helium-argon system of Evans, Watson and Truitt. The only differences between the predictions is the value of the Knudsen and ordinary diffusion coefficients, the gas properties, and the mole fraction range.

Finally, as an additional practical application for an air-water vapor system, applications to radial and linear two-phase heat pipes have been performed. Again, data for these configurations are not available, but this problem is of considerable interest in the verification of codes such as TOUGH2 since the problem can be solved with ordinary differential equations in radial (Doughty and Pruess, 1991a) or linear (Udell and Fitch, 1985) coordinates.

3.1 Evans, Watson, and Truitt Data

Evans, Watson, and Truitt (1962, 1963) obtained advection-diffusion data for a helium-argon system in a low-permeability graphite. The general configuration is shown in Figure 4. Essentially pure helium is present on one side, while essentially pure argon is present on the other; the exact mole fractions are dependent on the test and are given in Evans, Watson, and Truitt. In the present data-model comparison, predictions for the ADM and the DGM as implemented in TOUGH2 are given. In addition, other predictions from the DGM are also sometimes shown. These predictions, which are based on equations given by Mason and Malinauskas (1983), are approximate since simplifications were made in the numerical integration, such as assuming a linear variation of molecular densities. Therefore, exact agreement between the DGM and the implementation in TOUGH2 is not expected.

All these predictions are made with no adjustable constants, including the DGM predictions. As discussed in Section 2.3, the parameters are consistent between the two models and the values used in this comparison are listed in Table 1. The porosity-tortuosity factor for this graphite medium is exceptionally low at 1.42×10^{-4}. The ordinary and Knudsen diffusion coefficients for the DGM were measured for the graphite in independent tests. Since the ADM only uses a single Klinkenberg parameter, the DGM values for helium and argon are averaged for input to the ADM. The DGM predictions are made from the theory, not by curve-fitting the data.

3.1.1 Combined Advection and Diffusion

The first case is the most general situation of combined advection and diffusion. In this series of tests, the pressure difference across the test section was varied while maintaining the same average value. The individual fluxes of helium and argon across the low-permeability graphite test section were recorded at steady-state conditions. The predicted individual and net mole fluxes as a function of pressure difference are shown in Figures 5 and 6 for the DGM and ADM, respectively.

In Figure 5, DGM predictions of the mole fluxes are shown for the TOUGH2 implementation. DGM predictions are also given by Mason and Malinauskas (1983) but are not shown in the present figure since they are essentially the same as the TOUGH2-DGM results. The TOUGH2-DGM predictions compare quite well with the data for the individual mole fluxes of helium and argon as well as the net flux, including the variation with pressure difference.

Figure 6 presents the results for the ADM. The ADM predictions do not compare favorably with the data. Errors of a factor of 2 are noted for the individual fluxes with corresponding differences in the net flux. While the general trends are observed, the detailed variation is not well reproduced by the ADM approach.

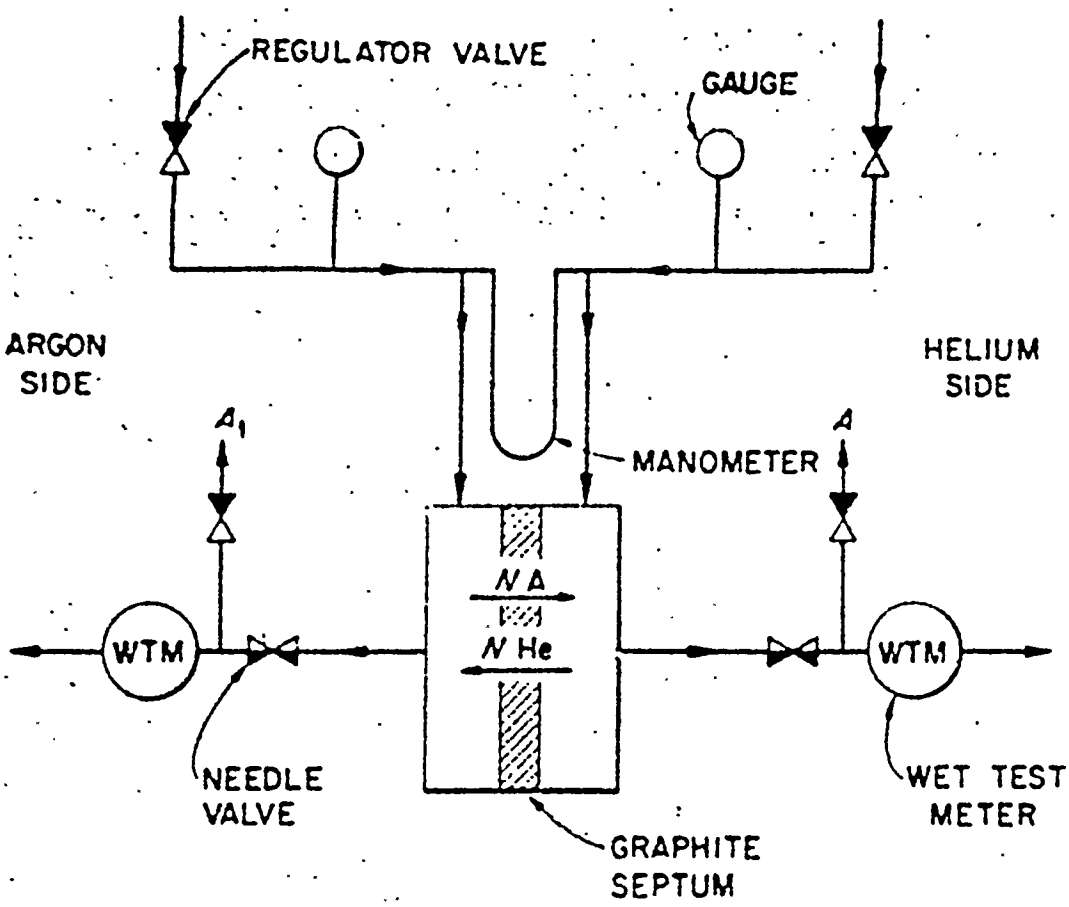

Figure 4
Schematic of Low-Permeability Graphite Experiment of Evans, Watson, and Truitt (from Evans, Watson, and Truitt, 1962)

Table 1
Parameters for He-Ar Data-Model Comparison

Graphite Permeability	2.13×10^{-18} m^2
Graphite Thickness	0.00447 m
D_{12} (at 1 atm)	1.06×10^{-8} m^2/s
D_{HeK}	3.93×10^{-8} m^2/s
D_{ArK}	1.24×10^{-8} m^2/s
Helium Viscosity	$198. \times 10^{-7}$ Pa-s
Argon Viscosity	$226. \times 10^{-7}$ Pa-s
Klinkenberg Parameter, He	3.65×10^{5} Pa
Klinkenberg Parameter, Ar	1.32×10^{5} Pa
Klinkenberg Parameter, ADM	2.48×10^{5} Pa
Gas Viscosity (constant)	$228. \times 10^{-7}$ Pa-s

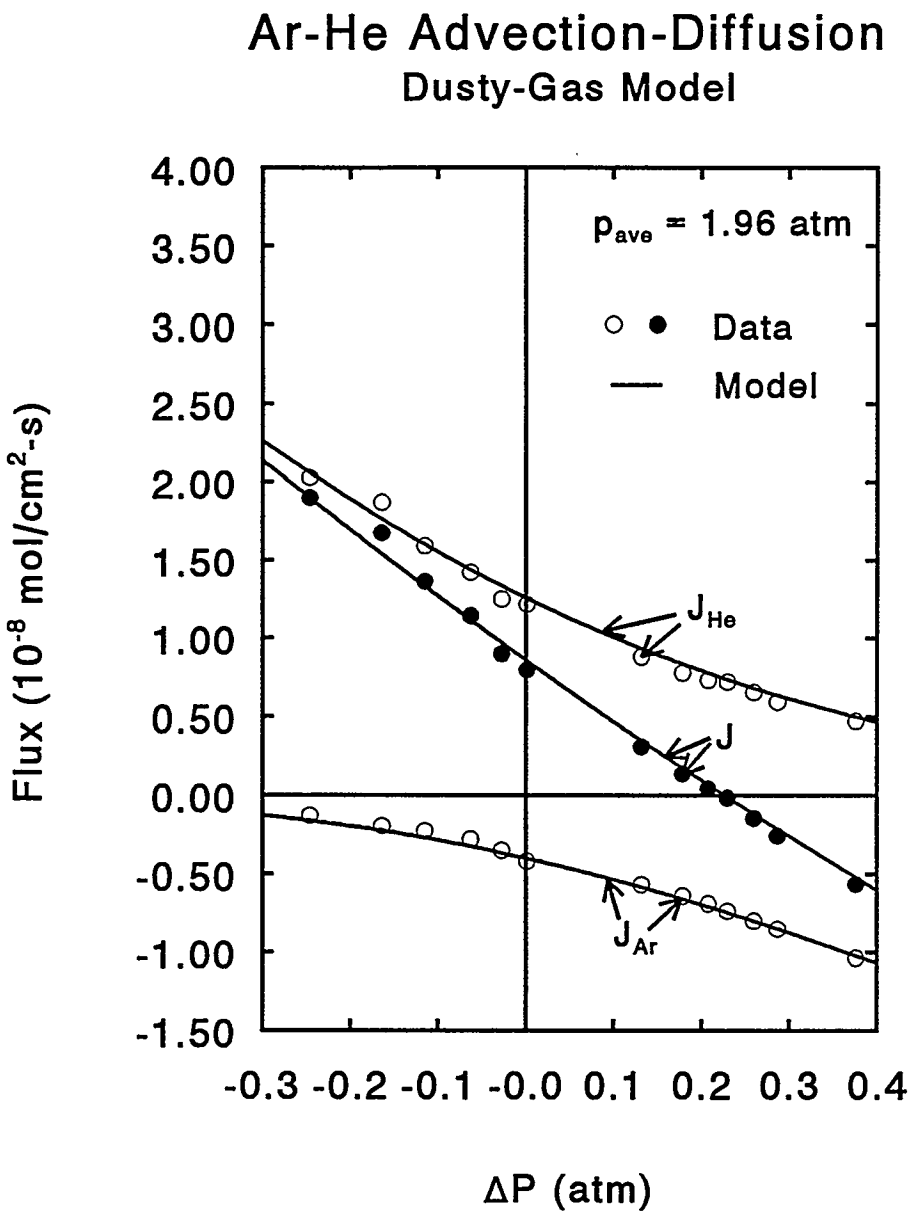

Figure 5
Combined Advection and Diffusion - DGM Data-Model Comparison

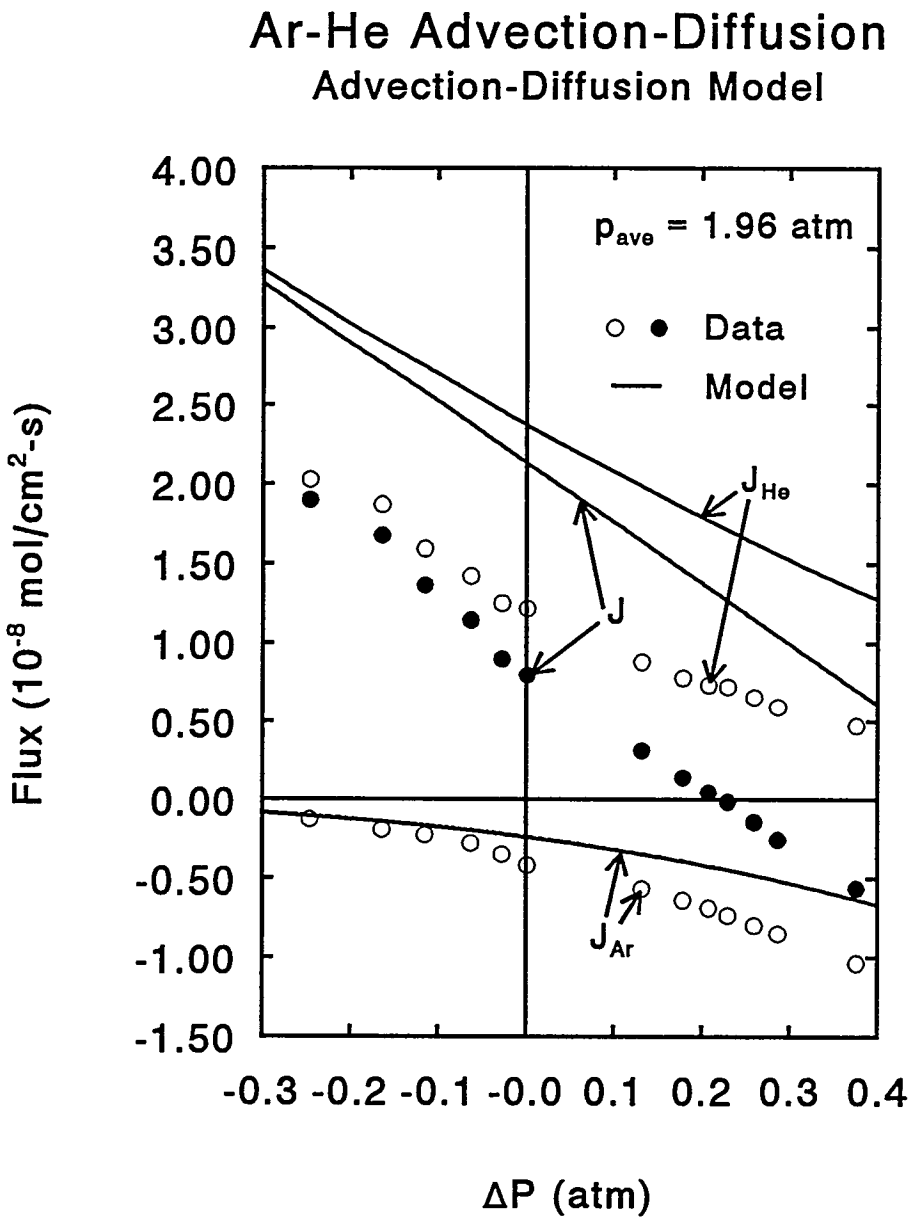

Figure 6
Combined Advection and Diffusion - ADM Data-Model Comparison

Since the advection formulations are equivalent as shown earlier, the differences must be due to the diffusion components. Two limiting cases of the test will be examined further. The first situation is for zero pressure difference, such that there is only diffusion. The second case is for zero net mole flux which is similar to what might be expected in a closed volume such as a heat pipe. Each case is discussed below.

3.1.2 Zero Pressure Difference

The second data-model comparisons considers zero pressure difference, or uniform pressure, conditions such that there is no advection, only diffusion. From Graham's laws, if only diffusion is occurring, the ratio of the mole fluxes is given by the inverse of the square root of the molecular masses, or

$$- J_1/J_2 = (m_2/m_1)^{1/2} . \qquad (54)$$

In this case, the ratio of the mole fluxes is always equal to the square root of the molecular weights independent of the diffusion regime. The ratio is the same in the Knudsen regime per Graham's law of effusion (equation 10) as in the ordinary diffusion regime per Graham's law of diffusion (equation 15). Based on the molecular weights of helium (m=4.00) and argon (m=39.944), the mole flux ratio of helium to argon should be about 3.16.

Figure 7 compares the data with the predictions from the ADM, the DGM, and the TOUGH2 implementation of the DGM (TOUGH2-DGM) as a function of the average pressure. Helium mole flux is positive, while argon mole flux is negative. The mole flux data for both gases increases with increasing pressure, eventually leveling off. The DGM predictions presented are based on expressions presented by Mason and Malinauskas (1983). The DGM, and the TOUGH2 implementation, predict the variation of the data quite well. The ratio of the mole fluxes is about 3.16 consistent with the theoretical ratio given above. In contrast, the ADM predicts a constant mole flux value unlike the data. As shown in Section 2.1, the mass fluxes of the two components are equal in the ADM, so the mole flux ratio is simply the ratio of the molecular weights, or about 10, whereas the ratio of the data is about 3.16. The ADM overpredicts the helium mole flux by about a factor of about 2, and underpredicts the argon mole flux by a factor of about 1.5-2. The ADM, which in this case is simply Fick's Law, does not predict the correct gas diffusion values or trends for this simple diffusion-only case.

The constant flux for the ADM can be explained by looking at the formulation. In the ADM, only ordinary or Fickian diffusion is important for zero pressure difference conditions; Knudsen diffusion is not invoked through the Klinkenberg factor since there is no pressure difference and no advective flow. For the ADM, the mass flux due to ordinary diffusion is given by

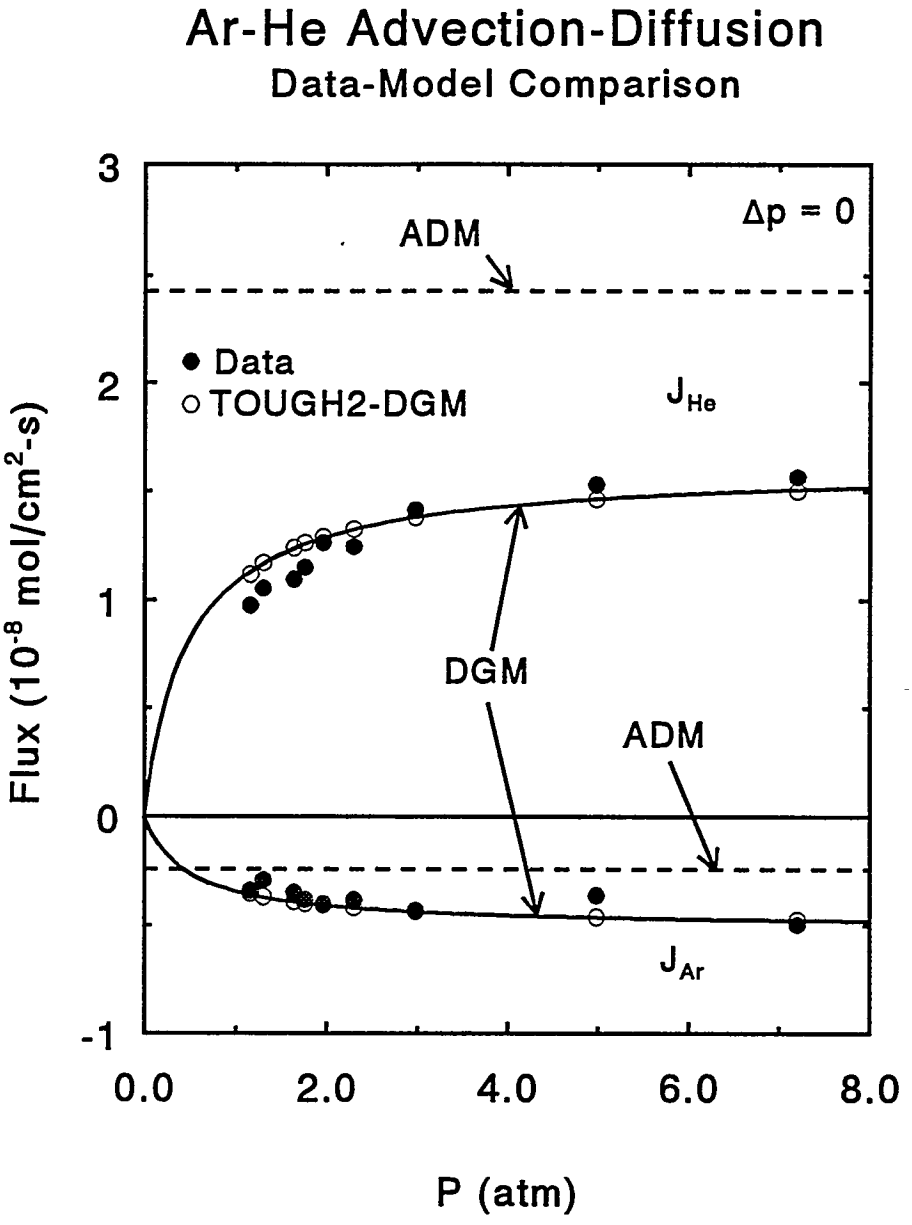

Figure 7
Zero Pressure Difference Data-Model Comparison

$$F_{1\ diffusion}^{ADM} = - D_{12}\rho_g \nabla\omega_1 \tag{55}$$

and the diffusion coefficient, D_{12}, for isothermal conditions is inversely proportional to pressure, or

$$D_{12} = \frac{D_{12}^0}{P} \tag{56}$$

where D_{12}^0 is the value at standard conditions. From the above two equations, for a perfect gas, the gas density increases with pressure while the diffusion coefficient decreases with pressure. Therefore, the ADM mass flux and mole flux for pure diffusion of perfect gases is constant as a function of pressure.

3.1.3 Zero Net Mole Flux

The final case simulates what would occur in a closed volume such as a heat pipe, where the total mole fluxes of the helium and argon components are equal, or $J_{He} = - J_{Ar}$. In this situation, diffusion and advection balance each other resulting in a zero net mole flux. The predicted flux corresponding to this condition, and the pressure difference across the low-permeability graphite associated with it, are compared to the experimental data.

Figure 8 shows the predicted mass flux with zero net mole flux for the ADM, the DGM, and the TOUGH2 implementation of the DGM along with the data as a function of the average pressure. The TOUGH2 implementation of the DGM compares well with the DGM curve. The DGM predictions, including TOUGH2-DGM, compare reasonably well with the experimental data including the variation of flux with pressure. In contrast, the ADM predicts a constant mole flux as a function of pressure similar to the zero pressure difference case. The ADM predictions are about 20% to 50% too high depending on the pressure; the higher error is for the lower pressures.

Figure 9 presents the data for the pressure difference across the low-permeability graphite sample and the model predictions. The pressure difference is that required for equal and opposite mole fluxes across the graphite. The TOUGH2-DGM predictions agree with the DGM and reasonably well with the data. The DGM predicts a maximum pressure difference at an average pressure of about 1 atmosphere; the data are not sufficient to resolve this behavior. The shape of the DGM pressure difference curve is due to the dominance of Knudsen diffusion pressure drop at low pressures and the dominance of advection pressure drop at higher pressures. The ADM consistently overpredicts the pressure difference by a factor of 2 or more and does not have the predicted shape from the DGM.

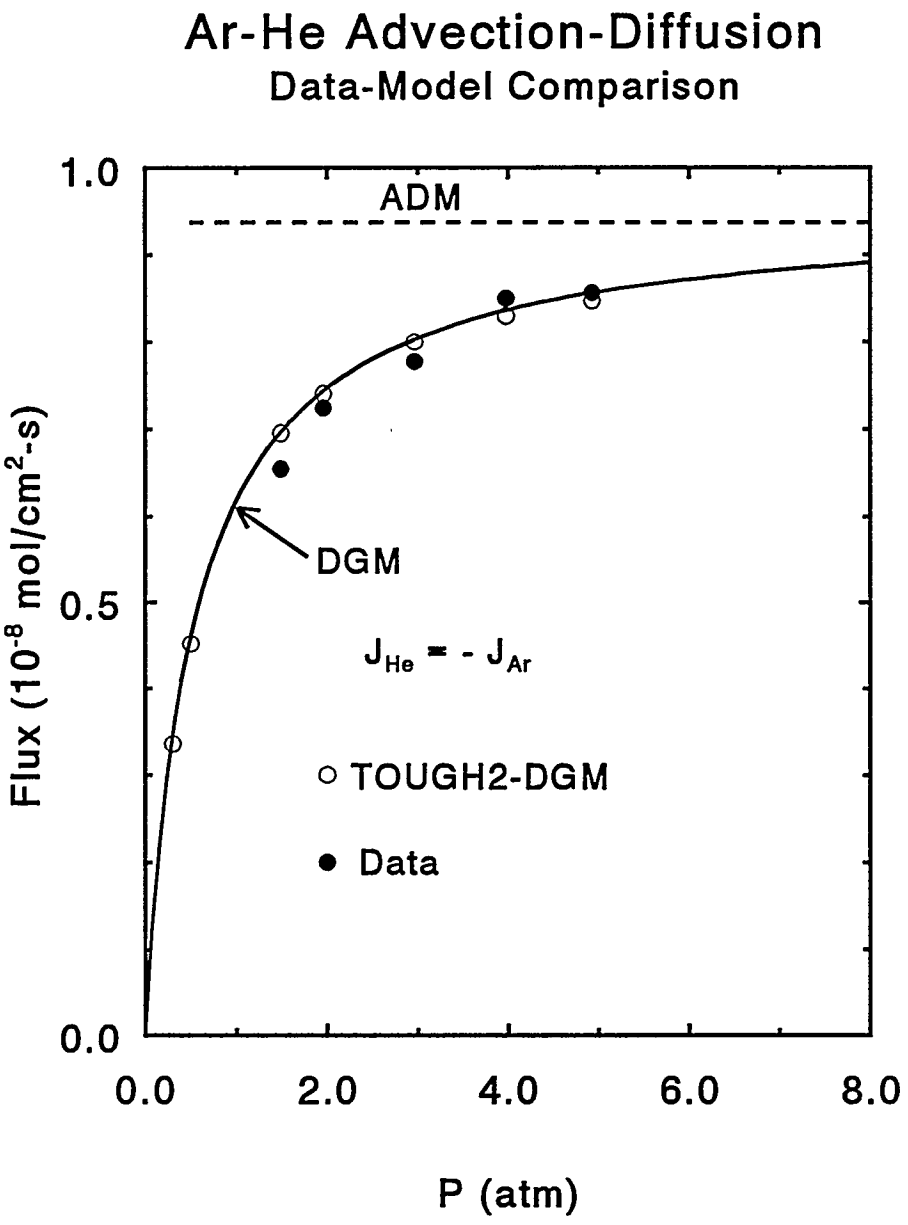

Figure 8
Zero Net Mole Flux - Flux Data-Model Comparison

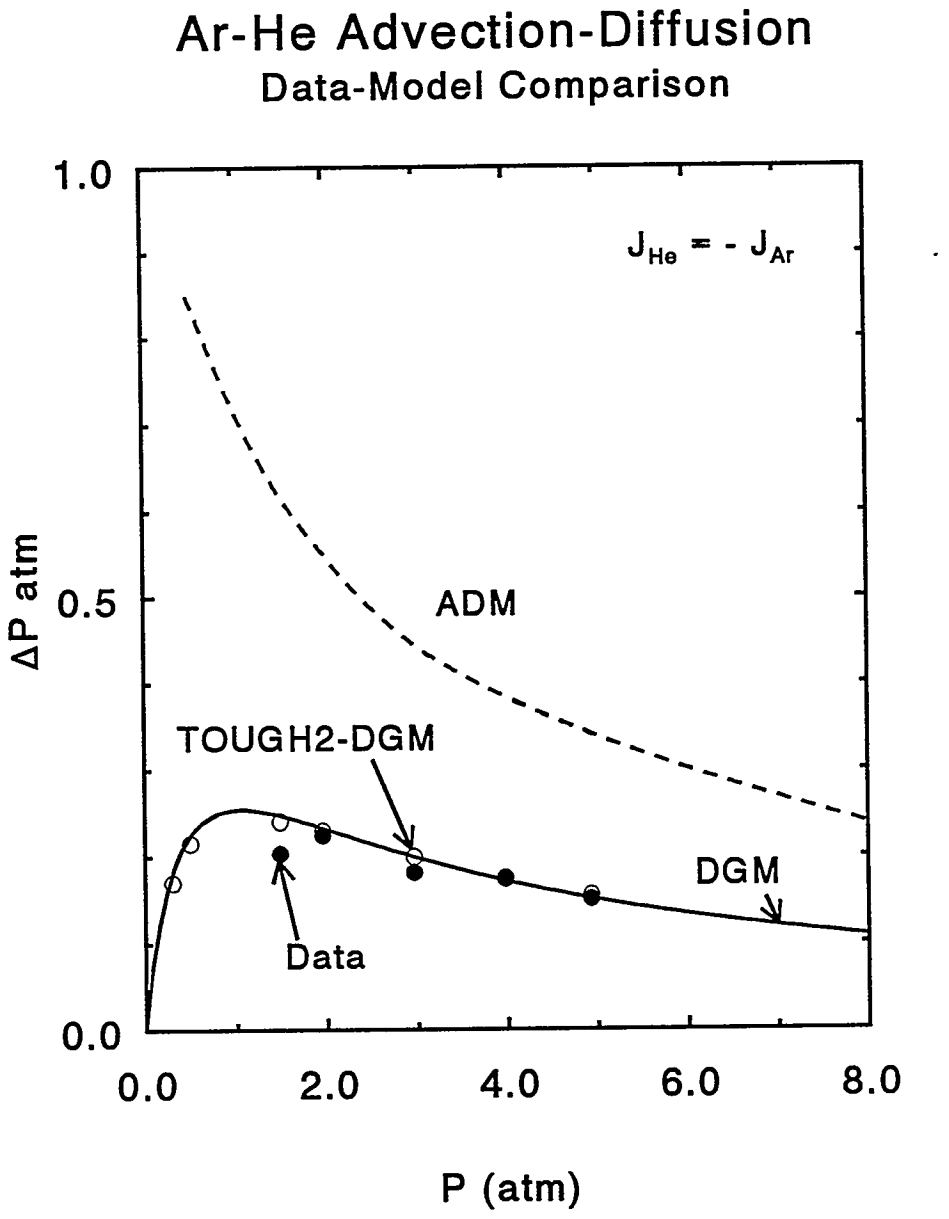

Figure 9
Zero Net Mole Flux - Pressure Difference Data-Model Comparison

3.2 Air-Water Vapor System

Predictions for an air-water vapor system for the experimental configuration of Evans, Watson, and Truitt have been performed for both models and are presented in this section. Only model differences are given; there are no data available for comparison. The parameters used for these predictions are summarized in Table 2. As discussed in the Appendix, the Knudsen diffusion coefficients simply scale by the square root of the ratio of temperature over the molecular weight. The air and water vapor values are scaled from the helium and argon values given in Table 1. The ordinary diffusion coefficient is based on a value of 2.13×10^{-5} m^2/s at 1 bar and 0°C, which was scaled to the pressure and temperature conditions given in Table 2. The effective diffusion coefficient for the porous medium is based on the porosity-tortuosity factor for the graphite medium as given by Evans, Watson, and Truitt (1962); the resulting value is given in Table 2. The mole fraction range is the maximum range for the pressure and temperature conditions. Pure air is imposed on one side, while the other side is air essentially saturated with water vapor at 1.96 atmospheres and 25° C, resulting in an air mole fraction of 0.986 (air mass fraction of 0.991).

Due to the large air mole fraction, the mole fluxes for air and water vapor are shown separately. Figure 10 gives the air fluxes for the system. The predictions for the ADM and the DGM are essentially identical on this plot. The differences near zero pressure difference are shown in Figure 11. The DGM gives smaller values for the air and water vapor mass fluxes than the ADM. The magnitude of the zero-pressure-difference mole flux for air is slightly larger (about 10%) for the DGM than the ADM, although the flux is generally overwhelmed by any advective contribution. Figures 11 and 12 show the water vapor mole fluxes for both models. The ADM predicts greater water vapor mole fluxes than the DGM. The ratio of the water vapor fluxes is given in Figure 13, indicating that the differences between the formulations may be greater than a factor of 1.5 for the conditions analyzed which increases with increasing pressure difference and decreasing flux values.

3.3 Radial Air-Water Heat Pipe

A two-phase radial air-water heat pipe problem was chosen for comparison of the DGM and the ADM because it is a sample problem for the TOUGH2 code (Pruess, 1991), has an ordinary differential equation similarity solution (Doughty and Pruess, 1991a), and has application to the Yucca Mountain nuclear waste repository. Application of the DGM to this two-phase system presents some additional complications, such as the appropriate interface terms, and numerical weighting issues. In addition, analysis of the heat pipe problem involves the prediction of diffusion coefficients where there are no data; the earlier two cases relied on measured diffusion parameters for ordinary and Knudsen diffusion. Thus, this application also involves practical aspects of the DGM.

Table 2
Parameters for Air-Water Vapor Model Comparison

Graphite Permeability	2.13×10^{-18} m^2
Graphite Thickness	0.00447 m
Pressure	1.96 atmospheres
Temperature	25 °C
D_{12} (at 1 atm)	3.50×10^{-9} m^2/s
$D_{\text{Water Vapor,K}}$	1.85×10^{-8} m^2/s
$D_{\text{Air,K}}$	1.46×10^{-8} m^2/s
Klinkenberg Parameter, Water Vapor	7.9×10^{4} Pa
Klinkenberg Parameter, Air	1.25×10^{5} Pa
Klinkenberg Parameter, ADM	1.25×10^{5} Pa

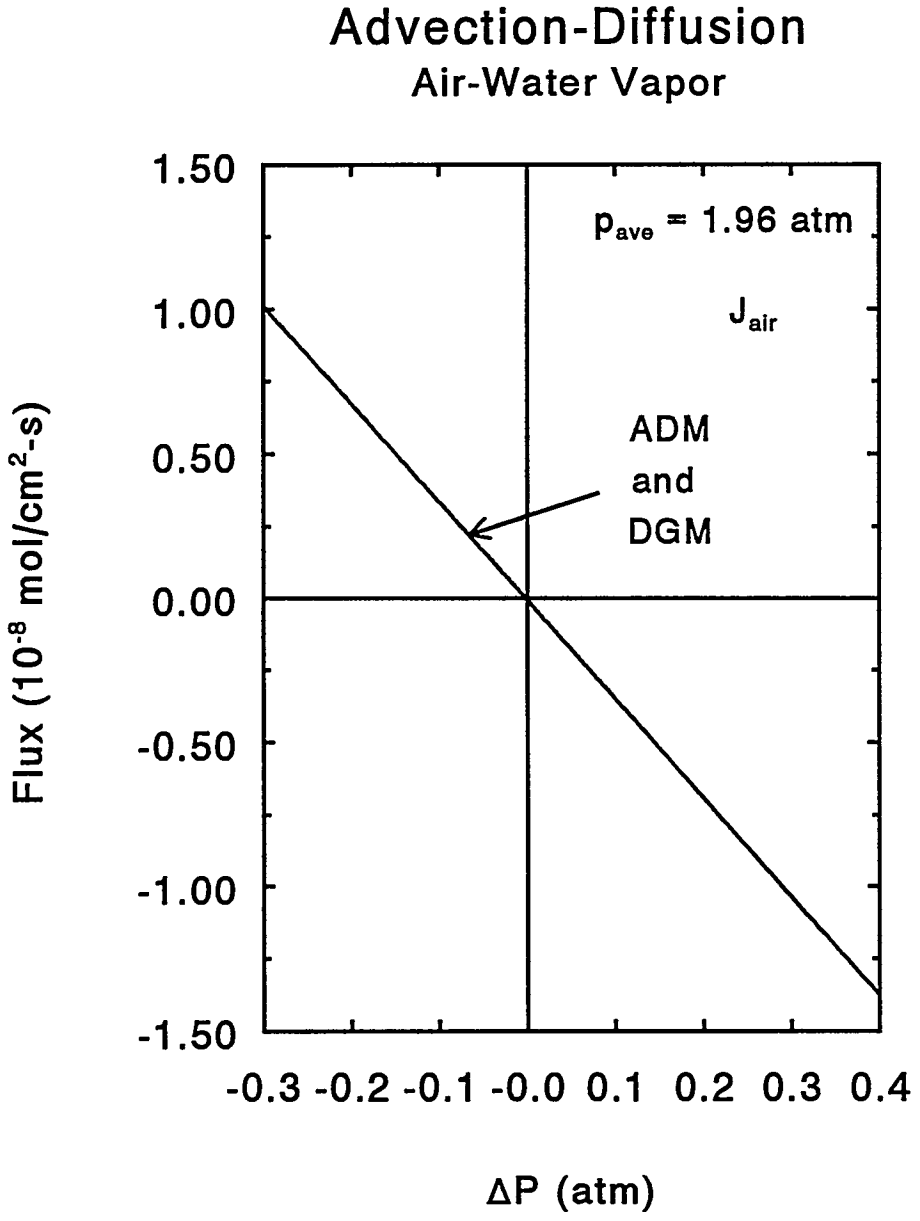

Figure 10
Combined Advection and Diffusion - Air Flux Model Comparison

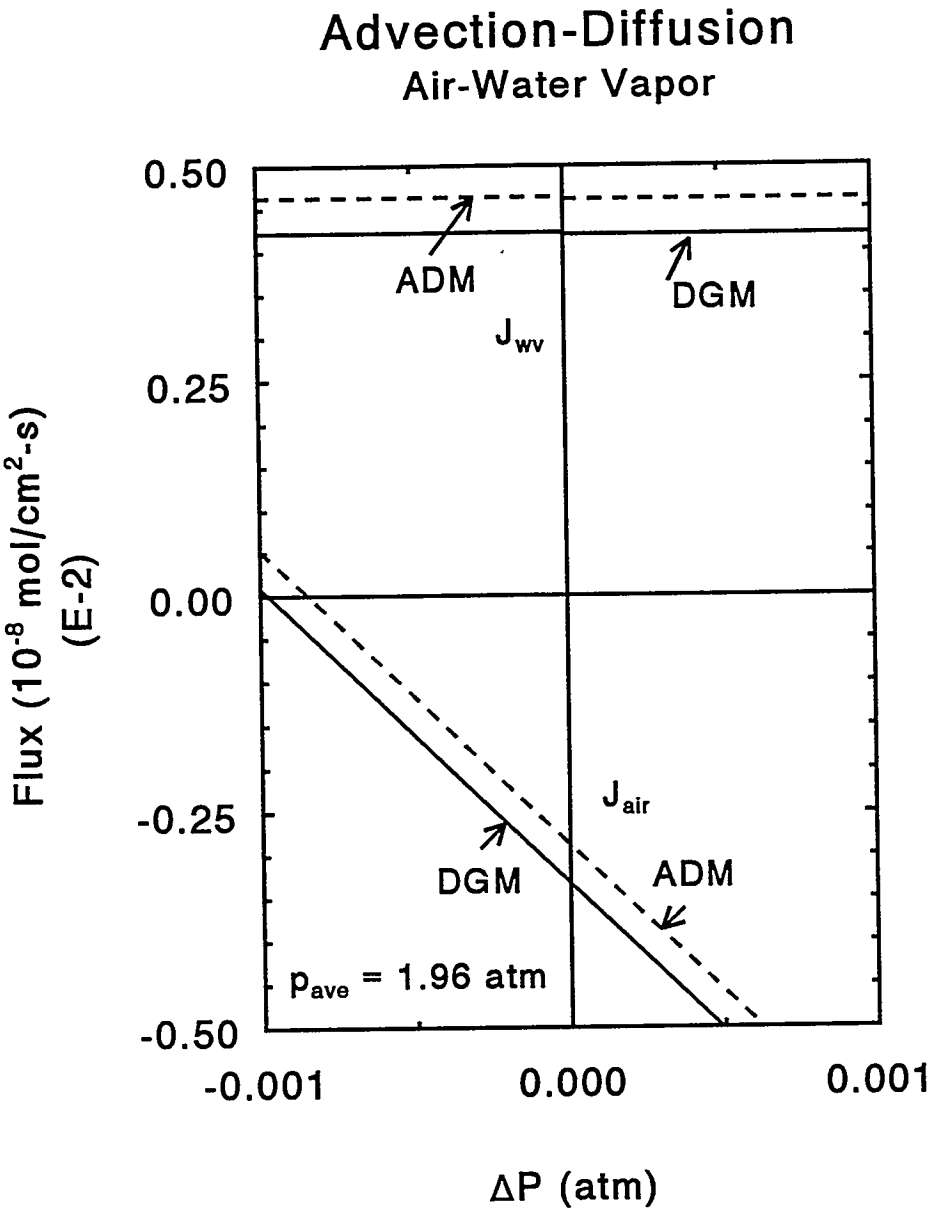

Figure 11
Combined Advection and Diffusion - Near-Zero ΔP Air and Water Flux Model Comparison

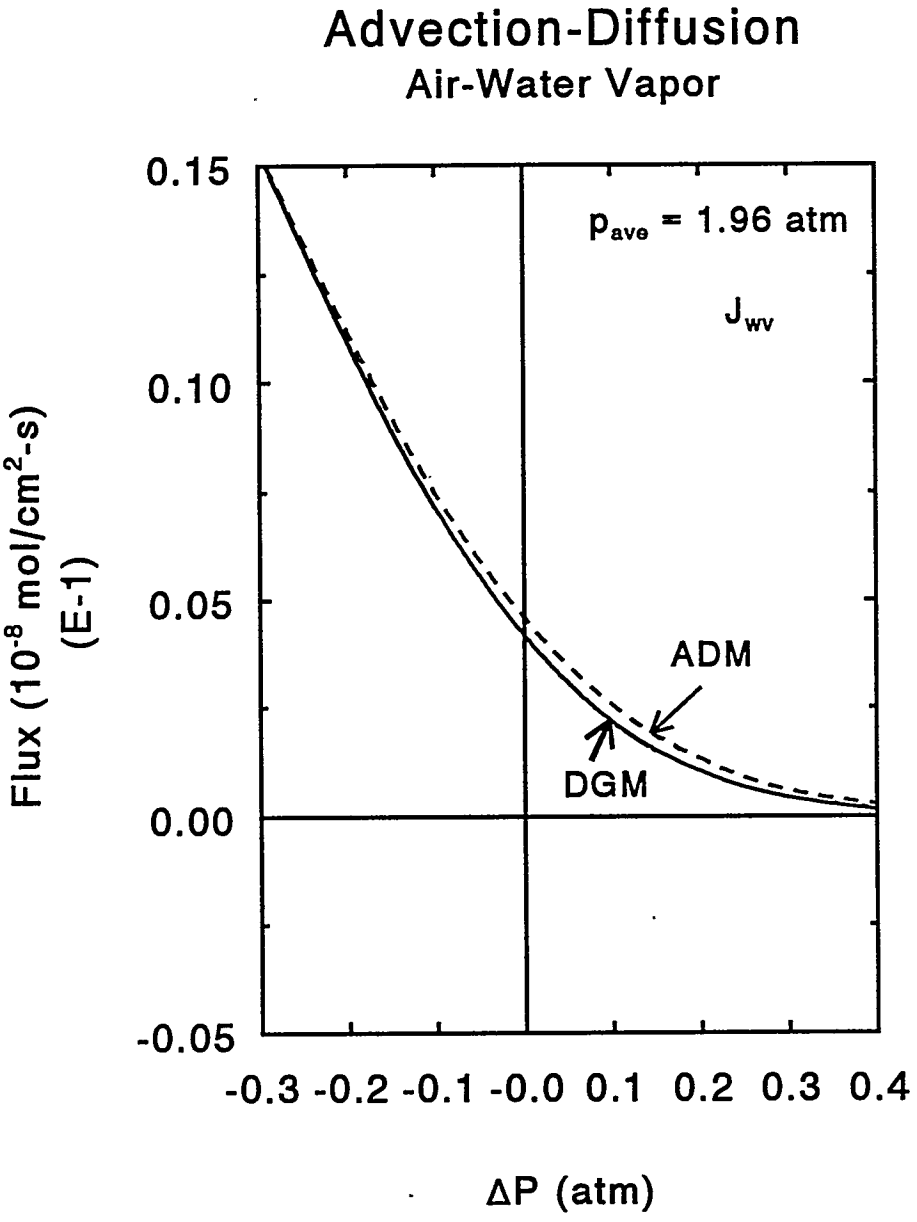

Figure 12
Combined Advection and Diffusion - Water Vapor Flux Model Comparison

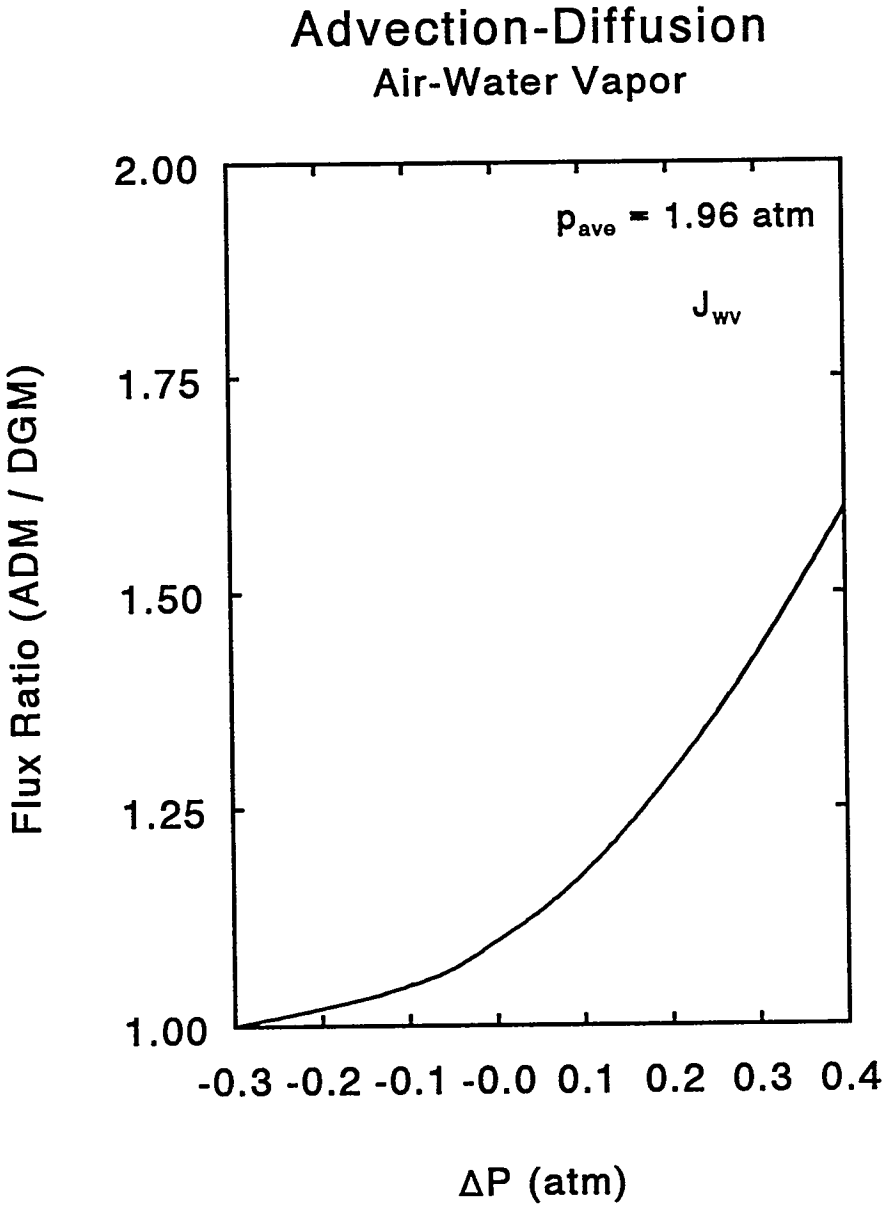

Figure 13
Combined Advection and Diffusion - Water Vapor Flux Ratio

The radial heat pipe problem is simply a one-dimensional radial problem with heat added at the center as shown schematically in Figure 14 as applied to Yucca Mountain. As the heat source temperature increases, the zone surrounding the heat source dries out, and conduction is the primary heat transfer mode. In the heat pipe region, water is evaporated and steam and air are advected radially outward. Because the temperature decreases radially outward, this water vapor condenses, and capillary forces transport the water back towards the evaporation region. Further out, heat transfer is again primarily by conduction.

Typical results, and comparison of TOUGH2 results with the similarity solution of Doughty and Pruess (1991a), are shown in Figure 15 where the thermodynamic parameters are presented as a function of the similarity variable, $r/t^{1/2}$. The single set of results actually include the time and space variation through the similarity variable. Thus, for a given value of the similarity variable, as time increases the appropriate radial distance also increases.

The input variables for this problem, including the geometry, are taken directly from Pruess (1991) as summarized in Table 3. The binary diffusion parameters from Doughty and Pruess (1991b) have been used. Unfortunately, the Klinkenberg factor was not included. For the present analysis, a correlation of the Klinkenberg parameter for air as a function of intrinsic permeability by Heid et al. (1950) was used as presented by Thorstenson and Pollock (1989), or

$$b_{air} = 0.11 k^{-0.39} \tag{57}$$

where b is in Pa and k is the intrinsic permeability in m^2. For an intrinsic permeability of 2. x 10^{-14} m^2, the Klinkenberg parameter is 24 kPa for air. As discussed in the Appendix, the Klinkenberg parameter is inversely proportional to the molecular weight, and the appropriate value for water vapor is 15 kPa. The average value of 19.5 kPa was used in the ADM predictions.

As discussed in the Appendix, the Knudsen diffusion coefficients needed for the DGM can be estimated from the Klinkenberg parameters, or

$$D_{iK} = k b_i / \mu_i \, . \tag{58}$$

The predicted Knudsen diffusion coefficients are 2.6 x 10^{-5} and 3.3 x 10^{-5} m^2/s for air and water vapor, respectively.

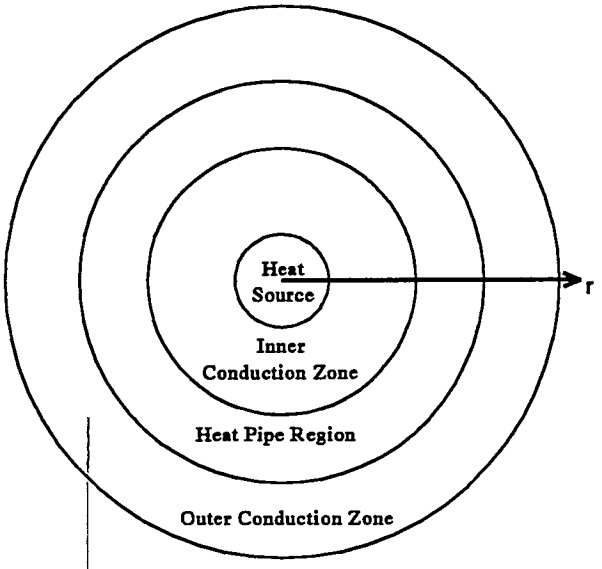

Figure 14
Schematic of Radial Heat Pipe
(after Doughty and Pruess, 1991a)

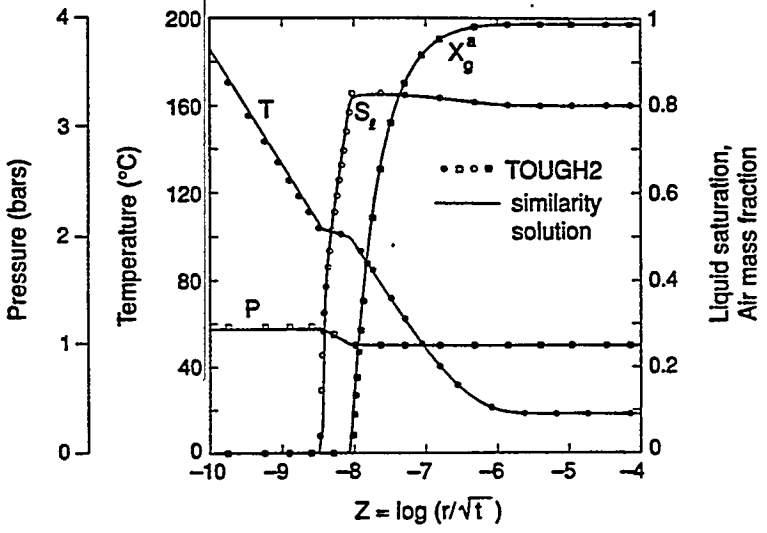

Figure 15
Typical Radial Heat Pipe Results
(from Pruess, 1991)

Table 3
Parameters for Radial Air-Water Heat Pipe Model Comparison

Initial Pressure	10^5 Pa
Initial Temperature	18 °C
Initial Gas Saturation	0.20
Heat Flux	667 W/m^2
Permeability	2.0×10^{-14} m^2
Porosity	0.10
Tortuosity	0.5
D_{12} (at 10^5 Pa, 0°C)	2.6×10^{-5} m^2/s
$D_{\text{Water Vapor,K}}$	3.3×10^{-5} m^2/s
$D_{\text{Air,K}}$	2.6×10^{-5} m^2/s
Klinkenberg Parameter, Water Vapor	15. kPa
Klinkenberg Parameter, Air	24. kPa
Klinkenberg Parameter, ADM	19.5 kPa

The numerical implementation issues of a two-phase system involve specification of the appropriate effective diffusion coefficients. As discussed by Mason and Malinauskas (1983), a porosity - tortuosity factor needs to be applied to the free space diffusion coefficient. In addition, for two-phase conditions, only the gas-phase area is appropriate, so the effective coefficient also includes the gas saturation. Therefore, consistent with the ADM as implemented in TOUGH2, the DGM effective diffusion coefficient is

$$D_{12,eff} = \tau \phi S_g D_{12} \tag{59}$$

although the form is not unequivocal (van Brakel and Heertjes, 1974).

Similarly, for the Knudsen diffusion coefficients, an effective value must be defined. Since the calculated Knudsen diffusion coefficients are based on a porous media correlation, the porosity - tortuosity factor is already taken into account as discussed by Thorstenson and Pollock (1989). For two-phase conditions, the effective diffusion coefficient will be less than the value for a gas-saturated medium. The gas saturation could be employed similar to the binary diffusion coefficient above. Gas saturation makes sense for the binary diffusion coefficient since the ordinary diffusion is dominated by molecule-molecule collisions, so the effective flow area is important. For Knudsen diffusion, however, wall-molecule collisions dominate. A weighting factor that considers the effects of the wall on flow is more appropriate. In the present case, the relative permeability, which implicitly includes the gas-phase flow area, has been chosen. The effective Knudsen diffusion coefficient is then the calculated value from the correlation times the relative permeability, or

$$D_{iK,eff} = k_{r,g} D_{iK} . \tag{60}$$

This definition is also consistent with the ADM formulation in TOUGH2 for two-phase flow. The advection expression for gas in TOUGH2, which includes the Klinkenberg factor, is multiplied by the gas-phase relative permeability for two-phase conditions similar to the expression above.

The Klinkenberg coefficient is also proportional to the square root of the temperature as discussed in the Appendix, so

$$D_{iK,eff} = k_{r,g} D_{iK} (T/T_{ref})^{1/2} . \tag{61}$$

Note that the ADM as implemented in TOUGH2 does not include this temperature effect in the Klinkenberg coefficient.

Finally, since Knudsen diffusion is a function of the pressure difference, the same numerical weighting used for advection should be employed for Knudsen diffusion. In the heat pipe simulations that follow, upstream weighting has been used for advection and for Knudsen diffusion.

Using the above approach, the ADM and the DGM were used to analyze the radial heat pipe out to a time of 10 years. The thermodynamic results are shown in Figure 16 for the two models; the results are essentially identical. The mass flow rates are shown in Figures 17 to 21, where a positive mass flow rate is to the right, or towards an increasing radius. Figure 17 shows the gas and liquid flow rates. Gas flows outward in the radial heat pipe, while liquid generally flows inward due to capillary pressure gradients. Again, the results from the two models are essentially the same. Figure 18 shows the air advection and diffusion mass fluxes. As expected, air is practically stagnant, as diffusion balances advection, and both mass fluxes are much smaller than the total gas flux. Although difficult to see, the air mass fluxes from the DGM are slightly smaller than the ADM; this difference is discussed below.

Figure 19 compares the vapor flow rates from the two models. For the ADM, practically all the gas flow is due to vapor advection; vapor diffusion is minimal. In contrast, for the DGM, while the gas flow is also predominantly vapor flow due to advection, there is an appreciable vapor diffusion component. This difference between the models is curious given the essentially identical total gas flux. The vapor diffusion flow for the DGM is broken down into Knudsen diffusion and ordinary diffusion components in Figure 20; the ADM ordinary diffusion flow is also included for comparison purposes. As can be seen, the ordinary diffusion component for both models are essentially the same. The differences seen in Figure 19 for the advective and diffusive flow rates are simply due to including Knudsen diffusion in the advective term in the ADM, while it is in the diffusion term in the DGM. Figure 21 shows a similar breakdown for the air flow rates for the DGM. The Knudsen diffusion flow rate accounts for the air flow rate differences noted above in Figure 18.

In summary, for the radial air-water heat pipe, the ADM and the DGM give essentially identical results for the radial heat pipe problem. The reason for this minimal difference is probably due two factors. First, the molecular weights of air and water vapor are fairly close, so minimal differences are expected as discussed earlier. Second, the problem is driven by heat input which causes evaporation of water which dominates the mass flow; air is essentially a passive component in this situation.

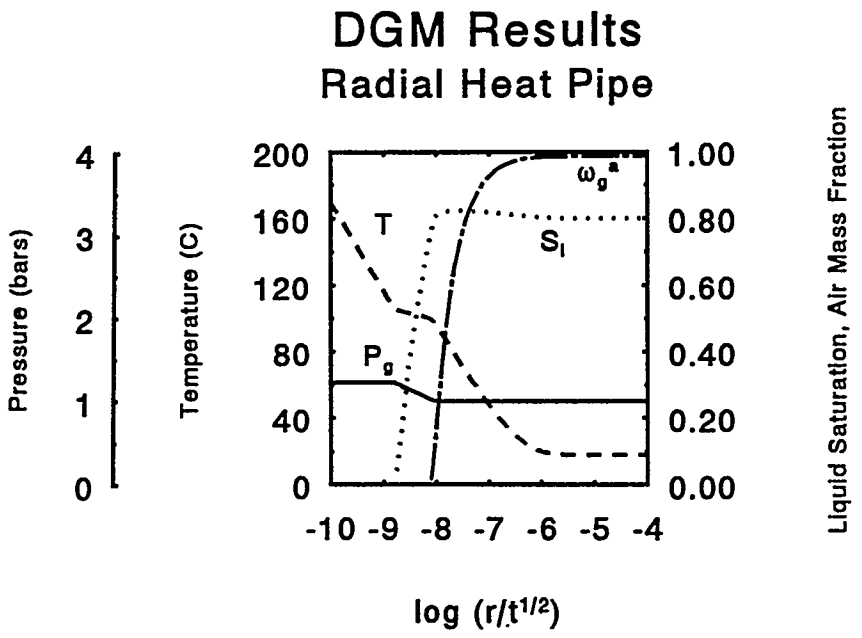

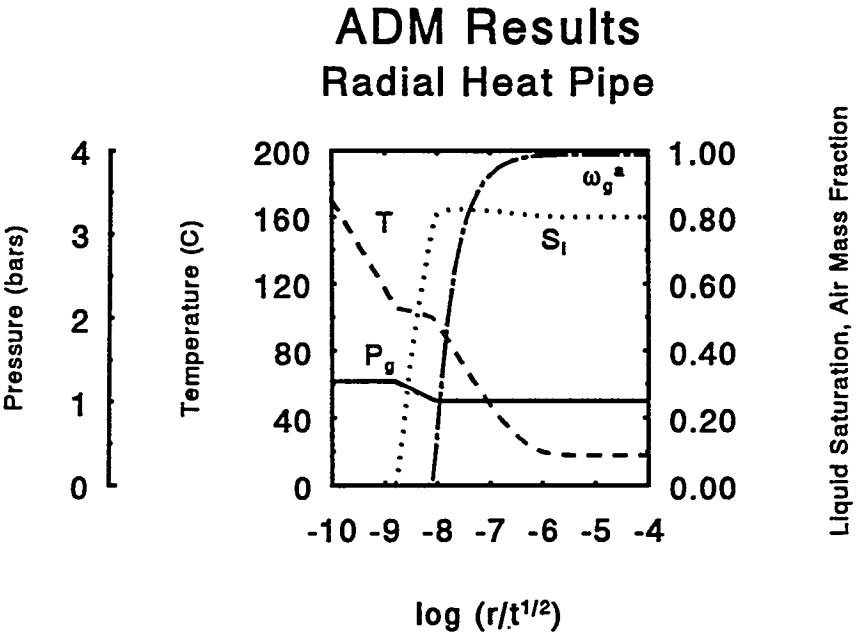

Figure 16
Radial Air-Water Heat Pipe
Model Comparison for Thermodynamic Variables

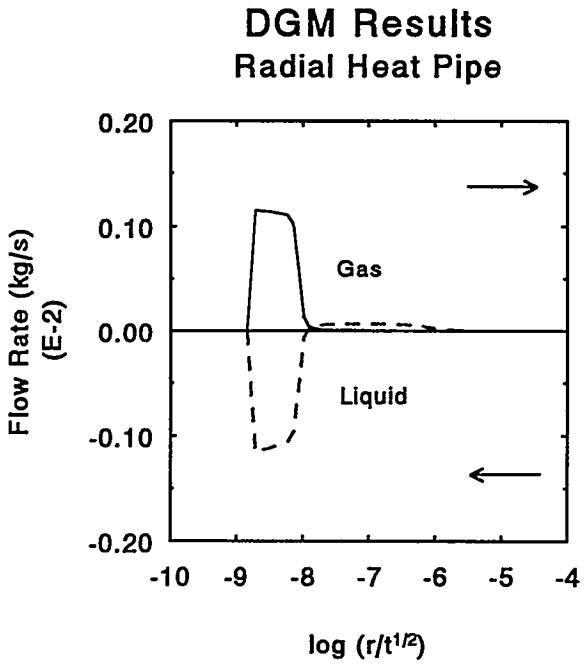

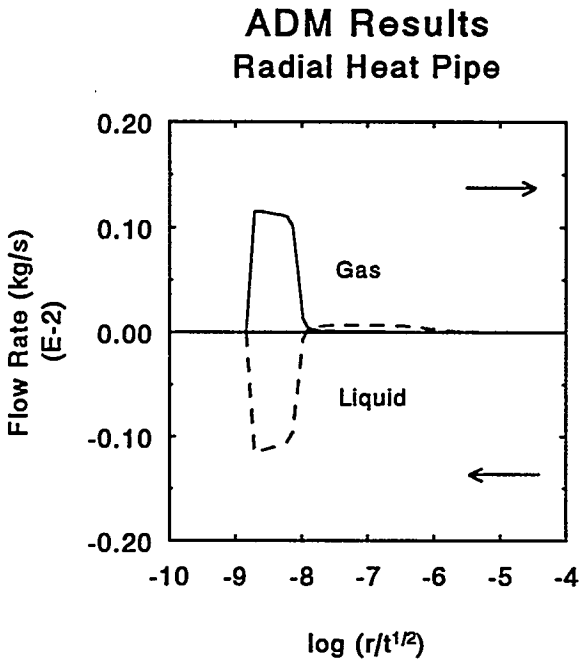

Figure 17
Radial Air-Water Heat Pipe
Comparison of Gas and Liquid Mass Flow Rates

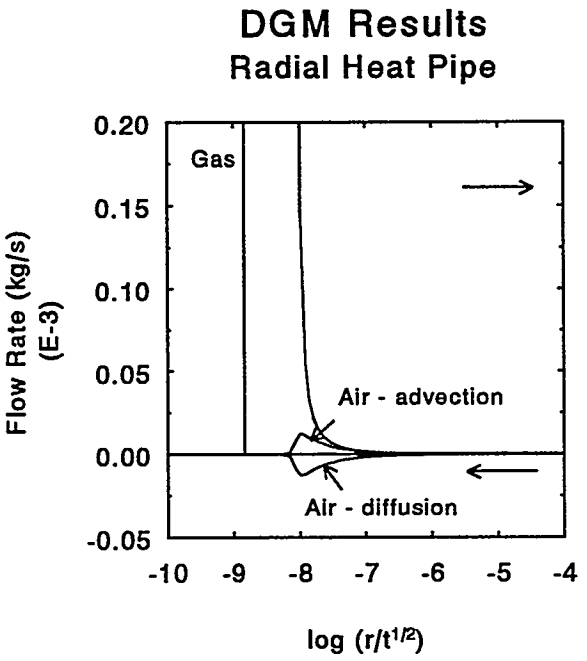

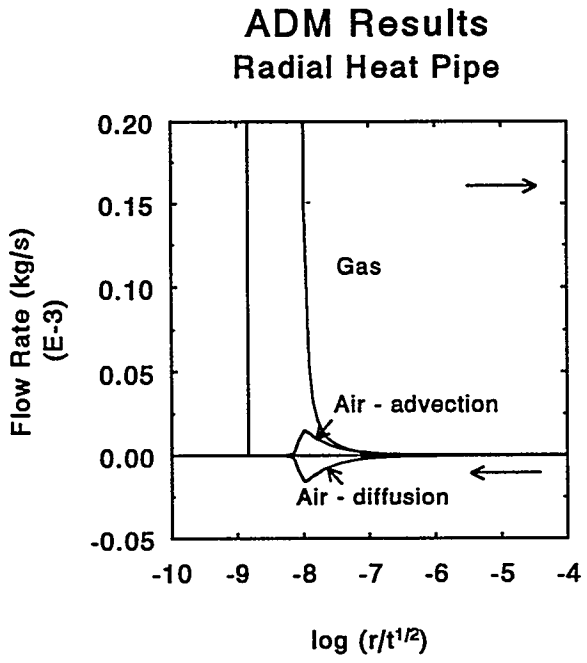

Figure 18
Radial Air-Water Heat Pipe
Comparison of Air Mass Flow Rate Components

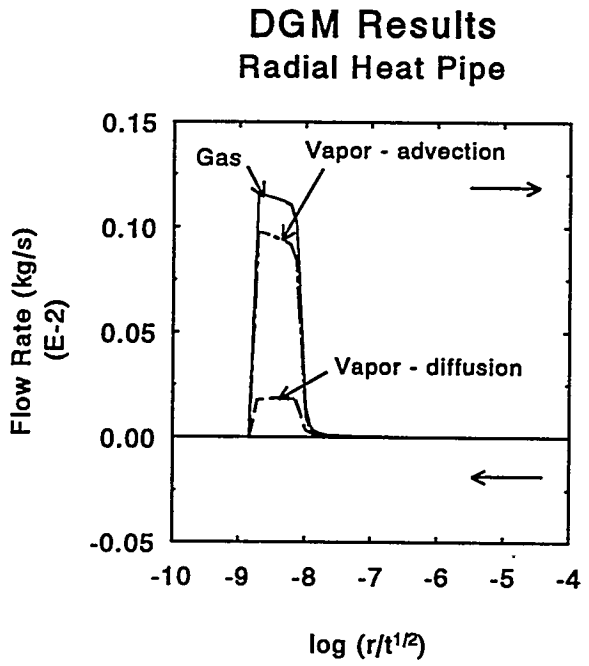

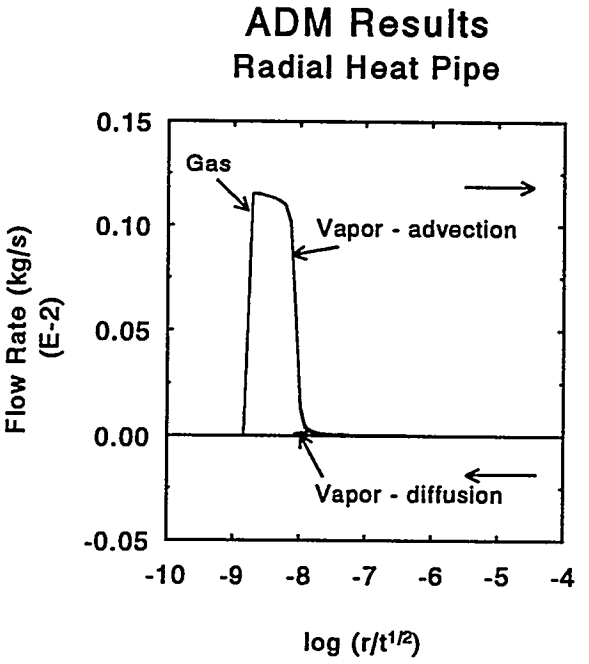

Figure 19
Radial Air-Water Heat Pipe
Comparison of Water Vapor Mass Flow Rate Components

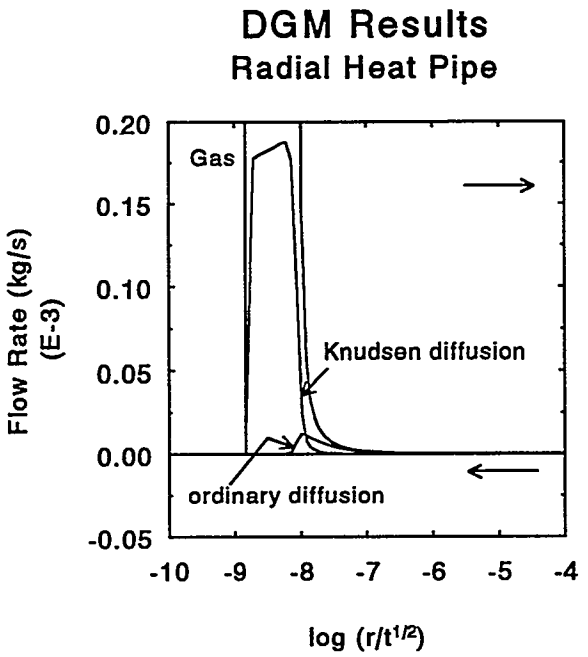

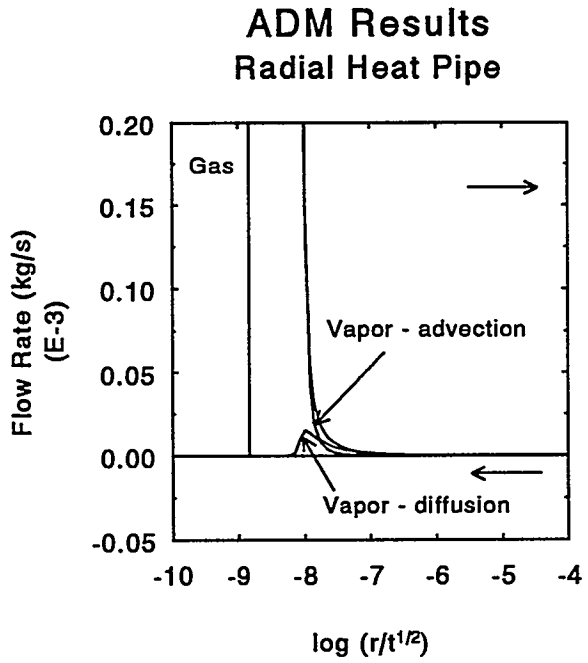

Figure 20
Radial Air-Water Heat Pipe
Comparison of Vapor Diffusion Flow Rate Components

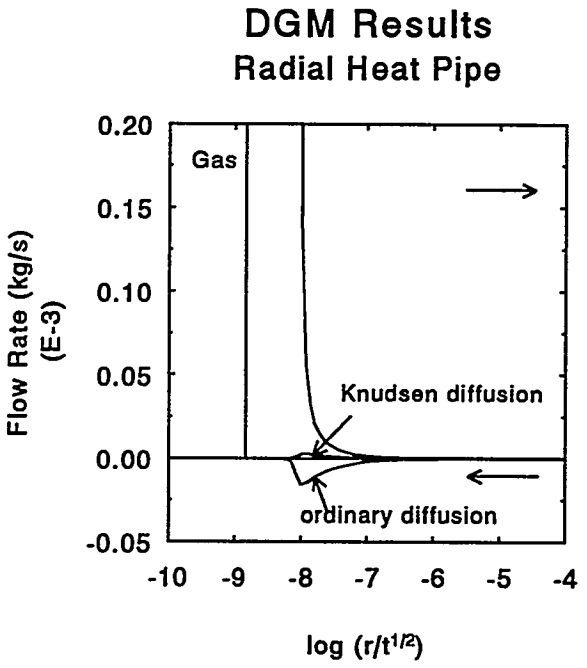

Figure 21
Radial Air-Water Heat Pipe
Breakdown of Air Diffusion Flow Rate Components for the DGM

3.4 Linear Air-Water Heat Pipe

The final problem chosen for comparison of the ADM and DGM is a two-phase linear air-water heat pipe problem as depicted in Figure 22. This problem was selected because it is a sample problem for the TOUGH code (Pruess, 1987), has an ordinary differential equation similarity solution (Udell and Fitch, 1985), and has application to the experimental configurations used to quantify enhanced vapor-phase diffusion. The same two-phase consideration discussed in the radial heat pipe problem (interface terms, numerical weighting) also apply to this application.

The linear heat pipe problem is simply a one-dimensional cartesian problem with heat added at one end and removed from the other. Unlike the radial problem, which is a developing transient problem, this problem is at steady-state. Water is evaporated at the hot end, and water vapor, or steam, flows to the cold end by advection and diffusion where it condenses. Water is then transferred back to the hot end by capillary forces. Air is essentially stagnant in the heat pipe, as advection and diffusion balance each other.

As discussed by Pruess (1987), the results from TOUGH (or TOUGH2) simulations will not be identical with the solution presented by Udell and Fitch (1985) because Udell and Fitch made a number of simplifying assumptions not made in TOUGH, such as constant properties. Figure 23 shows the agreement between TOUGH results and the solution of Udell and Fitch (Moridis and Pruess, 1992). As reported by Moridis and Pruess (1992), in order to resolve the differences, TOUGH was modified to use the same simplifications employed by Udell and Fitch resulting in excellent agreement.

Similar to the radial heat pipe, the input data file for TOUGH2 is based on the corresponding TOUGH Input file presented by Pruess (1987). The Klinkenberg factor was not included in the problem definition (the Klinkenberg factor was not a TOUGH input parameter; it was later added in TOUGH2). A value was calculated for the present problem based on the Heid et al. (1950) correlation discussed earlier. Problem parameters are summarized in Table 4.

Figure 24 compares the thermodynamic results for the ADM and the DGM. Note that the liquid saturations are scaled values relative to the residual liquid saturation. The predictions from both models are very similar except for the liquid saturation near 0. distance, which is higher for the DGM than the ADM. Otherwise, the temperature, gas pressure, liquid saturation, and air mole fraction in the gas phase are practically the same.

Figure 25 shows the gas and liquid flow rates as a function of distance for both models. Except for differences near 0.0 distance, and some minor differences near the right edge at about 2.15 meters, the mass flow rates are the same for the ADM and the DGM. Figure 26 presents the air advection and diffusion flow rates. The ADM air diffusion and advection flow rates are about a factor of 2 higher than the corresponding DGM flow rates. The water vapor advection and diffusion flow rates are summarized in Figure 27. The water vapor

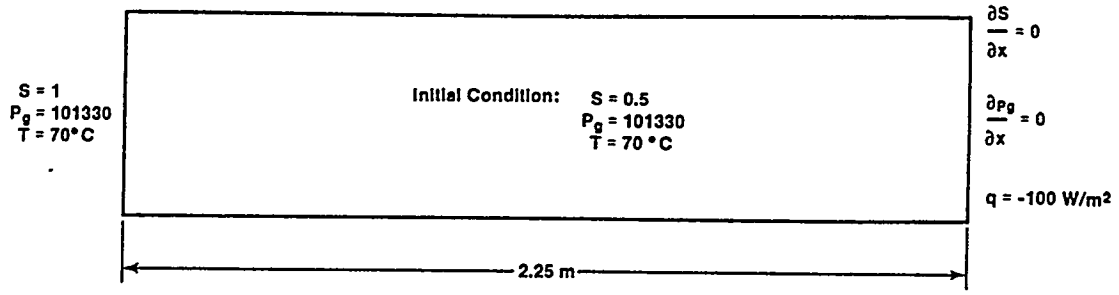

K_{sat} = 1.130 W/m - K $k = 10^{-12}$ m²
K_{dry} = 0.582 W/m - K $k_{rl} = S^3$
ϕ = 0.4 $k_{rg} = (1-S)^3$

$$P_c = \sigma (\phi/k)^{1/2}[1.417(1-S)-2.12(1-S)^2 + 1.263(1-S)^3]$$

Figure 22
Schematic of Linear Heat Pipe
(from Moridis and Pruess, 1992)

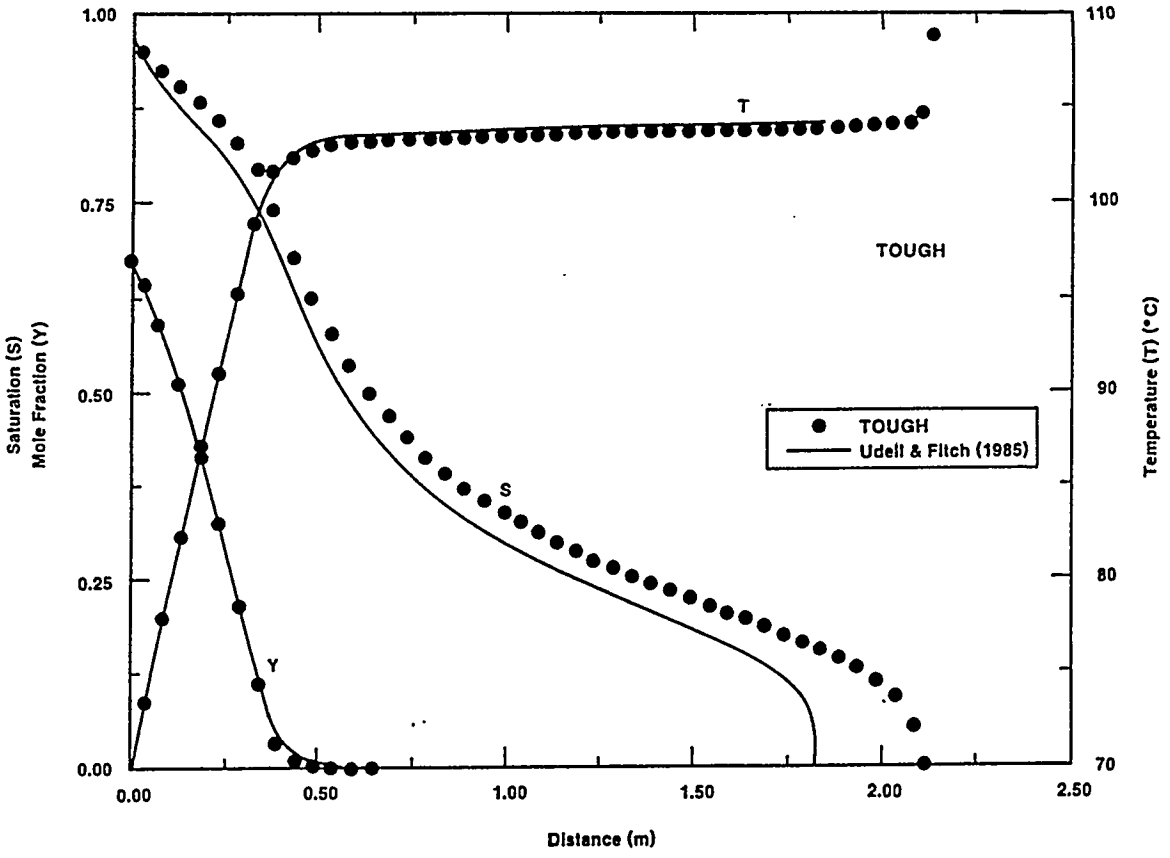

Figure 23
Comparison of Linear Heat Pipe Results from TOUGH with Udell and Fitch Solution (from Moridis and Pruess, 1992)

Table 4
Parameters for Linear Air-Water Heat Pipe Model Comparison

Initial Pressure	1.0133×10^5 Pa
Initial Temperature	70 °C
Initial Gas Saturation	0.50
Heat Flux	100 W/m^2
Permeability	10^{-12} m^2
Porosity	0.40
Tortuosity	0.5
D_{12} (at 10^5 Pa, 0°C)	2.6×10^{-5} m^2/s
$D_{\text{Water Vapor,K}}$	3.6×10^{-4} m^2/s
$D_{\text{Air,K}}$	2.9×10^{-4} m^2/s
Klinkenberg Parameter, Water Vapor	3.3 kPa
Klinkenberg Parameter, Air	5.3 kPa
Klinkenberg Parameter, ADM	4.3 kPa

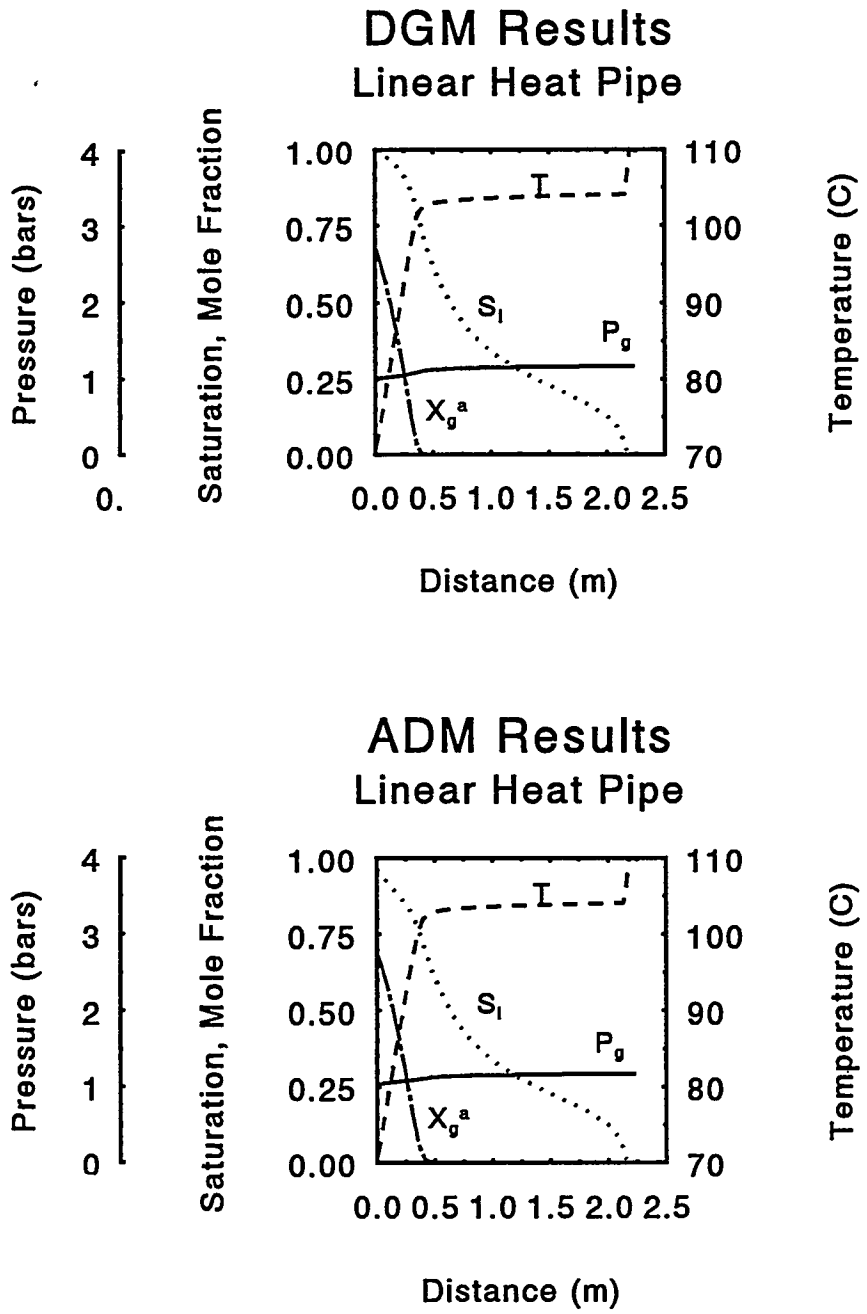

Figure 24
Linear Air-Water Heat Pipe
Model Comparison for Thermodynamic Variables

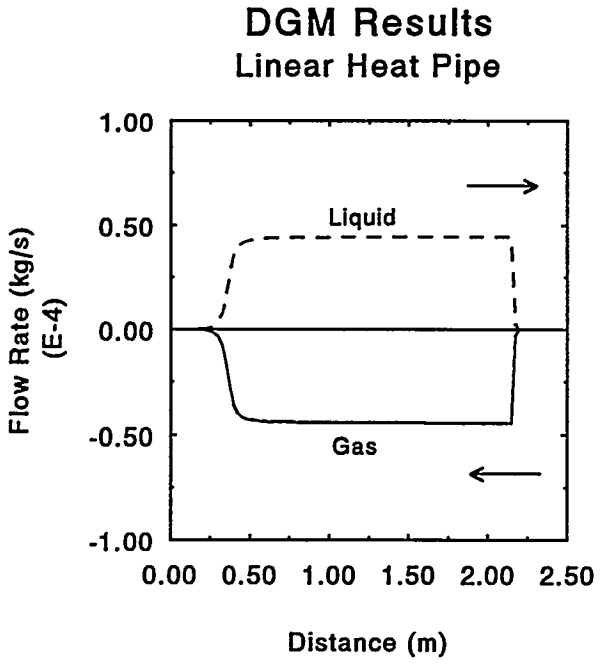

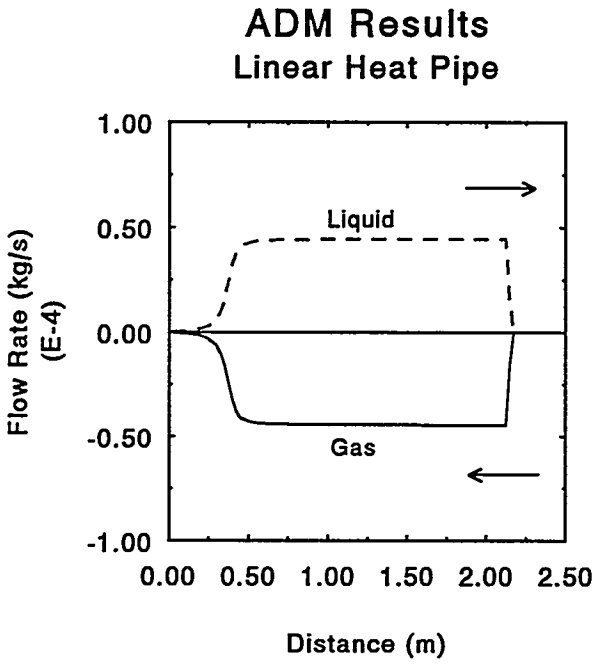

Figure 25
Linear Air-Water Heat Pipe
Comparison of Gas and Liquid Mass Flow Rates

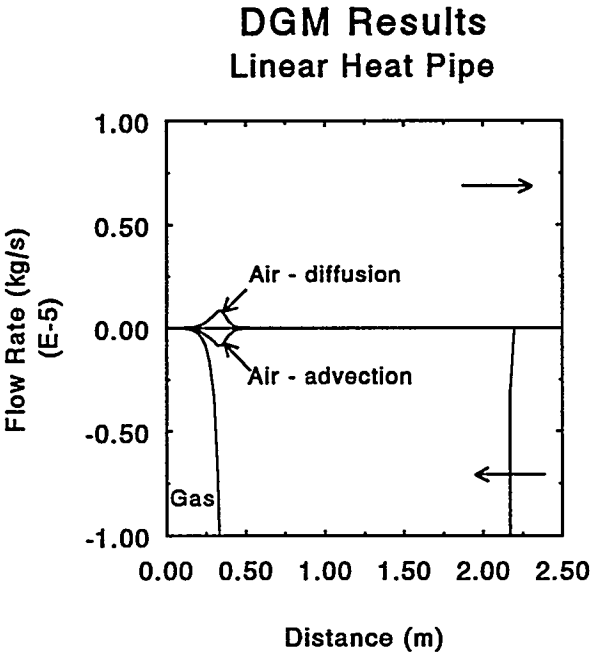

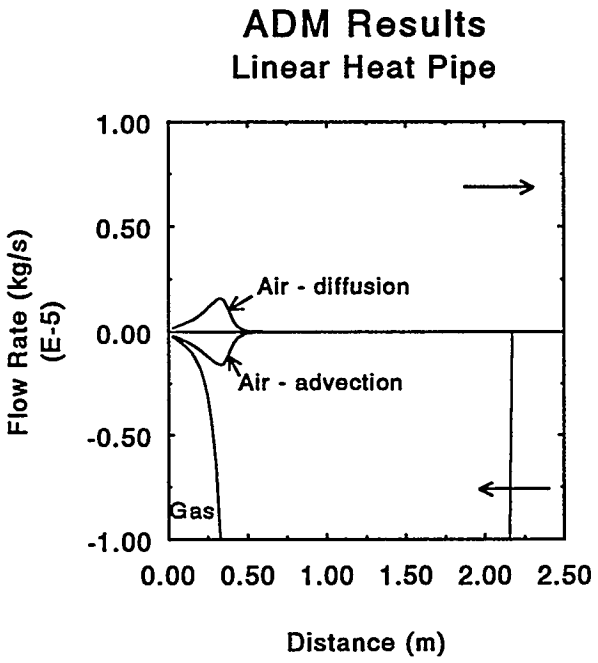

Figure 26
Linear Air-Water Heat Pipe
Comparison of Air Mass Flow Rate Components

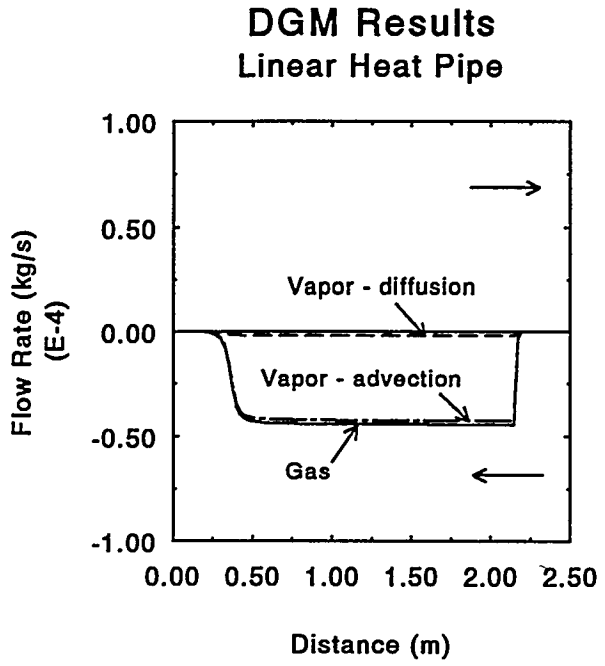

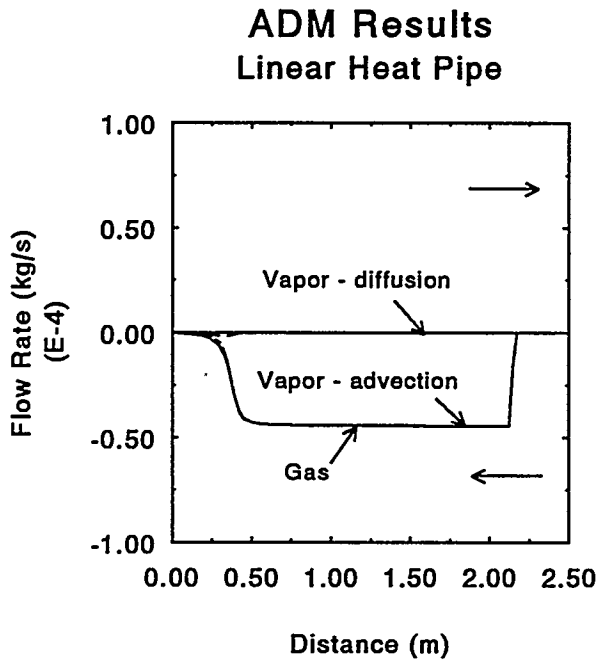

Figure 27
Linear Air-Water Heat Pipe
Comparison of Water Vapor Mass Flow Rate Components

diffusion flow rate is larger and the advection rate slightly smaller for the DGM than for the ADM. Figure 28 breaks down the diffusion flow rates into its various components. Most of the difference cited in Figure 27 is due to nomenclature in that Knudsen diffusion is included in the advective term in the ADM while it is a diffusion term in the DGM. However, comparison of the water vapor ordinary diffusion fluxes in Figure 28 reveals that the ADM values are significantly higher than the DGM flow rates by over a factor of 2. This behavior is consistent with the trend given in Figures 12 and 13, which indicated that the water vapor flux would be higher for the ADM than for the DGM, especially as the flux becomes small. Because the problem is driven by water (vapor and liquid) behavior, air reacts to the vapor behavior. Therefore, the air diffusive flux will also be higher for the ADM than for the DGM for the linear heat pipe problem.

The behavior of the diffusion fluxes given above for the linear heat pipe is different than for the radial heat pipe shown earlier. The reason is due to the different state of the problems. The radial heat pipe is a transient problem in which the phase change propagates radially with time. While the gas and liquid mass flow rates are very similar in magnitude as shown in Figure 17, there are significant differences at low flow rates. Thus, the net flux of water vapor never becomes "small" when diffusion is occurring. In the linear heat pipe, however, the problem is run to steady-state conditions, so the net flux becomes vanishingly small throughout the entire heat pipe. As shown earlier in Figures 12 and 13, the difference between the water vapor flux predicted by the ADM and the DGM increases as the net flux decreases; thus, a larger difference between the models is expected for the linear heat pipe than for the radial heat pipe.

Diffusion in the linear heat pipe occurs predominantly near the cold end due to air movement. Thus, the ADM mass flow rate is much higher than the DGM flow rate near the cold end, which in turn decreases the liquid saturation at the cold end (as noted in Figure 24). Overall, however, the linear air-water heat pipe shows minimal differences between the ADM and the DGM similar to the other air-water problems.

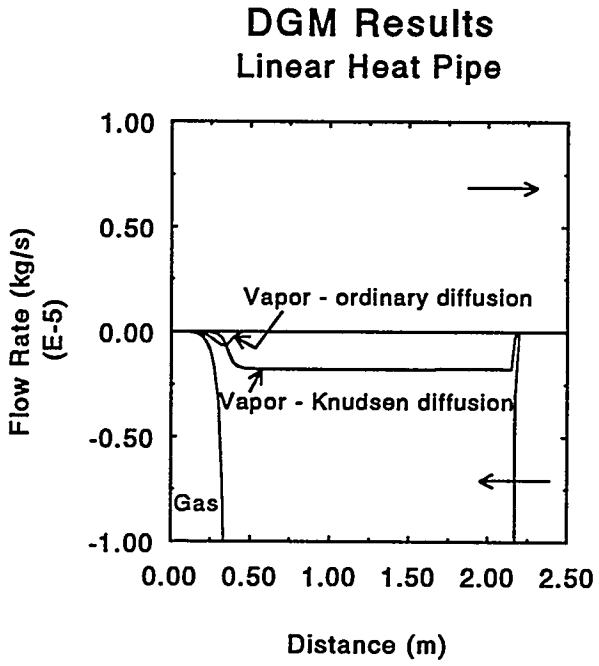

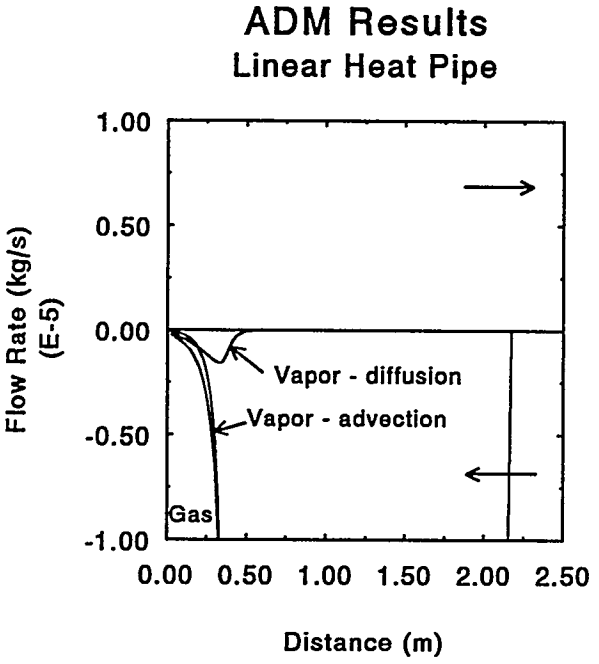

Figure 28
Linear Air-Water Heat Pipe
Breakdown of Water Wapor Diffusion Flow Rate Components

4.0 DISCUSSION

Two models for gas-phase diffusion and advection in porous media, the Advective-Diffusive Model (ADM) and the Dusty-Gas Model (DGM), have been reviewed. The ADM, as exemplified by the TOUGH2 computer code (Pruess, 1991), is widely used and simply adds advection calculated by Darcy's Law with a Klinkenberg coefficient to account for slip to ordinary diffusion calculated by Fick's Law for free-space with a porosity-tortuosity-gas saturation correction factor. The DGM is a more comprehensive model based on the kinetic theory of gases. The approach includes Knudsen and ordinary diffusion along with advection. Combination of the various mechanisms is performed in a detailed manner considering coupling between the various phenomena.

The results from these two models have been compared to the isothermal experimental data for He-Ar gas diffusion in a low-permeability graphite of Evans, Watson, and Truitt (1962, 1963). Data-model comparisons for mole fluxes have been made for combined advection and diffusion, pure diffusion ($\Delta p=0$), and zero net mole flux or closed-system behavior ($J_1=-J_2$). Additionally, data-model comparisons have been made for the pressure difference in the zero net mole flux case. In all four of these comparisons, the DGM is far superior to the ADM. The DGM correctly predicts data values and trends. In contrast, the ADM is in error by up to a factor of 2 or more compared to the data and does not capture many of the data trends. Based on these comparisons, Fick's Law must be defined relative to the mole-average velocity to calculate gas diffusion in porous media; the stationary coordinate definition used in the advective-dispersive formulation discussed here in inappropriate and may lead to significant errors in the component fluxes, especially for stagnant conditions. Similar conclusions were reached by Thorstenson and Pollock (1989).

Comparison of results from the ADM and the DGM have also been made for an isothermal air-water vapor system for the Evans, Watson, and Truitt experimental configuration. The results showed generally small differences in the flow rates between the two models.

A radial air-water heat pipe has also been analyzed with both models including a discussion of some of the issues associated with applying the DGM to a two-phase situation. The problem involves a two-phase air-water system with heat, advection, capillary transport, and diffusion under nonisothermal conditions. The results for the radial air-water heat pipe are essentially identical for the ADM and DGM predictions.

A linear air-water heat pipe was also considered. While the results are generally similar from the ADM and DGM, some differences exist in the saturations and ordinary diffusion flow rates which were not seen in the radial heat pipe. The different behavior is attributed to the difference in the state of the two heat pipe problems. The radial heat pipe is a transient problem, while the linear heat pipe is steady-state. Differences in the mass fluxes predicted by the ADM and DGM get larger as the water vapor flux decreases, which is exacerbated by the steady-state conditions of the linear heat pipe problem.

A number of other data-model comparisons have been done using the DGM. Gunn and King (1969) compared the DGM to simultaneous diffusion and advection in fritted glass, while Wong et al. (1975, 1976) used the DGM for analyzing combined diffusion, flow, and reaction of a ternary mixture in a porous catalyst. Hanley (1965) and Hopfinger and Altman (1969) both experimentally verified the DGM for thermal transpiration. Therefore, the DGM has been successfully tested in a number of diverse applications.

Phenomenologically, the DGM is superior to the ADM. The DGM provides a solid theoretical framework for the various mechanisms, and successfully reproduces data trends for a wide range of problem configurations. In contrast, the ADM, while conceptually appealing, does not reproduce the observed data trends in many situations.

From the results shown in the present study, the differences in model performance depend on the ratio of the molecular weights of the gases. In the case of helium and argon, the ratio is about 10, while the air-water vapor ratio is only about 1.6. In addition, as discussed earlier in Section 2.4 and as seen by Abriola et al. (1992), the differences between the two models depend on the media permeability. From Abriola et al. (1992), the DGM and ADM predict similar results for a high permeability soil ($3x10^{-10}$ m^2) but considerably different results for a low permeability soil (1.25×10^{-16} m^2). In an air-water vapor system or a high permeability media, the ADM may be adequate but, based on phenomenological considerations, the DGM is preferred. For other applications with a large difference in molecular weights, which include the helium - argon system or an air - VOC system, or for a low permeability media, the reliability of the ADM is questionable and the DGM is the obvious choice.

The use of the DGM is recommended over the ADM for gas-phase transport analysis in porous media. The data requirements for both models are the same, and no difference in computer time was noted for the present calculations. Additional data-model comparisons are needed for air-VOC systems and for multicomponent mixtures. In addition, data-model comparisons for actual soils including unsaturated conditions would be beneficial.

5.0 SUMMARY

In summary, the results from the current study comparing the Advective-Dispersive Model (ADM) and the Dusty-Gas Model (DGM) for combined advection and diffusion of gases in porous media are:

1. The DGM is superior to the ADM for combined advection and diffusion in porous media and is recommended. Based on the He-Ar data, the DGM successfully reproduces the data and trends, while the ADM is unsuccessful. Fick's Law must be defined relative to the mole-average velocity to calculate gas diffusion in porous media; the stationary coordinate definition used in some advective-dispersive formulations is inappropriate and may lead to significant errors in the component fluxes, especially for stagnant conditions.

2. For an air-water system, the differences between the two models are much smaller than the He-Ar system.

3. Differences between the ADM and DGM depend on the ratio of molecular weights of the diffusing gases. As the ratio of molecular weights increases, so does the difference between the ADM and DGM predictions. The ratio for the He-Ar system is about 10., while the ratio for the air-water vapor system is about 1.6. For other applications such as an air-VOC system, significant differences are possible.

4. Differences between the ADM and DGM depend on the permeability of the porous medium probably due to Knudsen diffusion. As the permeability decreases, the differences between the ADM and DGM increase.

5. Additional data-model comparisons are needed including air-VOC systems, multicomponent mixtures, and diffusion in actual soils including unsaturated conditions.

6.0 REFERENCES

Abriola, L.M., and G.F. Pinder (1985), "A Multiphase Approach to the Modeling of Porous Media Contamination by Organic Compounds - 1. Equation Development," Water Resourc. Res., Vol. 21, pp. 11-18.

Abriola, L.M., C.-S. Fen, and H.W. Reeves (1992), "Numerical simulation of unsteady organic vapor transport in porous media using the dusty gas model," Surface Contamination by Immiscible Fluids, Weyer, ed., Balkema, Rotterdam, pp. 195-202.

Adenekan, A.E., T.W. Patzek, and K. Pruess (1993), "Modeling of Multiphase Transport of Multicomponent Organic Compounds and Heat in the Subsurface: Numerical Model Formulation," Water Resour. Res., Vol. 29, pp. 3727-3740.

Bird, R.B., W.E. Stewart, and E.N. Lightfoot (1960), Transport Phenomena, John Wiley & Sons, New York.

Bixler, N.E. (1985), *NORIA - A Finite Element Computer program for Analyzing Water, Vapor, Air, and Energy Transport in Porous Media*, SAND84-2057, Sandia National Laboratories.

Cunningham, R.E., and R.J.J. Williams (1980), Diffusion in Gases and Porous Media, Plenum Press, New York.

Doughty, C., and K. Pruess (1991a), "A Similarity Solution for Two-Phase Water, Air, and Heat Flow near a Linear Heat Source in a Porous Medium," Int. J. Heat Mass Trans., pp. 1205-1233.

Doughty, C., and K. Pruess (1991b), "A Mathematical Model for Two-Phase Water, Air, and Heat Flow Around a Linear Heat Source Emplaced in a Permeable Medium," Heat Transfer - Minneapolis 1991, AIChE Symposium Series, No. 283, Vol. 87, pp. 256-265.

Evans, III, R.B., G.M. Watson, and E.A. Mason (1961), "Gaseous Diffusion in Porous Media at Uniform Pressure," J. Chem. Physics, Vol. 35, No. 6, pp. 2076-2083.

Evans, III, R.B., G.M. Watson, and E.A. Mason (1962), "Gaseous Diffusion in Porous Media. II. Effect of Pressure Gradients," J. Chem. Physics, Vol. 36, No. 7, pp. 1894-1902.

Evans, III, R.B., G.M. Watson, and J. Truitt (1962), "Interdiffusion of gases in a low permeability graphite at uniform pressure," J. Appl. Phys., Vol. 33, pp. 2682.

Evans, III, R.B., G.M. Watson, and J. Truitt (1963), "Interdiffusion of gases in a low permeability graphite. II. Influence of pressure gradients," J. Appl. Phys., Vol. 34, pp. 2020.

Falta, R.W., K. Pruess, S. Finsterle, and A. Battistelli (1995), *T2VOC User's Guide*, LBL-36400, Lawrence Berkeley Laboratory.

Farr, J.M. (1990), "Gaseous Transport of Volatile Organics in Porous Media: Comparison of Mathematical Models," in *Proceedings of the TOUGH Workshop*, K. Pruess, Editor, LBL-29710, Lawrence Berkeley Laboratory, pp. 21-28.

Finsterle, S., E. Schlueter, and K. Pruess (1990), *Exploratory Simulations of Multiphase Effects in Gas Injection and Ventilation Tests in an Underground Rock Laboratory*, LBL-28810, Lawrence Berkeley Laboratory.

Graham, T. (1833), "On the law of the diffusion of gases," Phil. Mag., Vol. 2, pp. 175, 269, 351, reprinted in "Chemical and Physical Researches," pp. 44-70, Edinburgh Univ. Press, Edinburgh, 1876.

Graham, T. (1846), "On the motion of gases," Phil. Trans. Roy. Soc., Vol. 136, pp. 573, reprinted in "Chemical and Physical Researches," pp. 44-70, Edinburgh Univ. Press, Edinburgh, 1876.

Gunn, R.D., and C.J. King (1969), "Mass Transport in Porous Materials under Combined Gradients of Composition and Pressure," AIChE J., Vol. 15, No. 4, pp. 507-514.

Hadley, G.R. (1982), "Theoretical Treatment of Evaporation Front Drying," Int. J. Heat Mass Transfer, Vol. 25, No. 10, pp. 1511-1522.

Hadley, G.R. (1985), *PETROS -- A Program for Calculating Transport of Heat, Water, Water Vapor and Air Through a Porous Material*, SAND84-0878, Sandia National Laboratories.

Hanley, H.J.M. (1965), "Experimental Verification of the 'Dusty-Gas' Theory for Thermal Transpiration," J. Chem. Physics, Vol. 43, No. 5, pp. 1510-1514.

Heid, J.G., J.J. McMahon, R.F. Nielson, and S.T. Yuster (1950), "Study of the Permeability of Rocks to Homogeneous Fluids," API Drilling and Production Practice, pp. 230-244..

Hopfinger, E.J., and M. Altman (1969), "Experimental Verification of the Dusty-Gas Theory for Thermal Transpiration through Porous Media," J. Chem. Physics, Vol. 50, No. 6, pp. 2417-2428.

Hoogschagen, J. (1953), "Equal pressure diffusion in porous substances," J. Chem. Phys., Vol. 21, pp. 2096.

Hoogschagen, J. (1955), "Diffusion in porous catalysts and adsorbants," Ind. Eng. Chem., Vol. 47, pp. 906.

Jackson, R. (1977), Transport in Porous Catalysts, Chem Eng. Monograph 4, Elsevier, New York.

Klinkenberg, L.J. (1941), "The Permeability of Porous Media to Liquids and Gases," API Drilling and Production Practice, pp. 200-213.

Lenhard, R.J., M. Oostrom, C.S. Simmons, and M.D. White (1995), "Investigation of density-dependent gas advection of trichloroethylene: Experiment and a model validation exercise," J. Contaminant Hydrology, Vol. 19, pp. 47-67.

Martinez, M.J. (1995a), *Formulation and Numerical Analysis of Nonisothermal Multiphase Flow in Porous Media*, SAND94-0379, Sandia National Laboratories.

Martinez, M.J. (1995b), *Mathematical and Numerical Formulation of Nonisothermal Multicomponent Three-Phase Flow in Porous Media*, SAND95-1247, Sandia National Laboratories.

Mason, E.A., R.B. Evans, III, and G.M. Watson (1963), "Gaseous Diffusion in Porous Media. III. Thermal Transpiration," J. Chem. Physics, Vol. 38, No. 8, pp. 1808-1826.

Mason, E.A., and A.P. Malinauskas (1964), "Gaseous diffusion in porous media. IV. Thermal diffusion," J. Chem. Phys., Vol. 41, pp. 3815.

Mason, E.A., and A.P. Malinauskas (1983), Gas Transport in Porous Media: The Dusty-Gas Model, Chem Eng. Monograph 17, Elsevier, New York.

Mason, E.A., A.P. Malinauskas, and R.B. Evans III (1967), "Flow and Diffusion of Gases in Porous Media," J. Chem. Physics, Vol. 46, No. 8, pp. 3199-3216.

Moridis, G.J., and K. Pruess (1992), *TOUGH Simulations of Updegraff's Set of Fluid and Heat Flow Problems*, LBL-32611, Lawrence Berkeley Laboratory.

Pruess, K. (1987), *TOUGH User's Guide*, NUREG/CR-4645, SAND86-7104, LBL-20700, US Nuclear Regulatory Commission.

Pruess, K. (1991), *TOUGH2 - A General-Purpose Numerical Simulator for Multiphase Fluid and Heat Flow*, LBL-29400, Lawrence Berkeley Laboratory.

Pruess, K., Editor (1995), *Proceedings of the TOUGH Workshop '95*, LBL-37200, Lawrence Berkeley Laboratory.

Pruess, K., and Y. Tsang (1993), *Modeling of Strongly Heat-Driven Flow Processes at a Potential High-Level Nuclear Waste Repository at Yucca Mountain, Nevada*, LBL-33597, Lawrence Berkeley Laboratory.

Thorstenson, D.C., and D.W. Pollock (1989), "Gas Transport in Unsaturated Zones: Multicomponent Systems and the Adequacy of Fick's Laws," Water Resourc. Res., Vol. 25, No. 3, pp. 477-507.

Tsang, Y.W., and K. Pruess (1990), *Further Modeling Studies of Gas Movement and Moisture Migration at Yucca Mountain, Nevada*, LBL-29127, Lawrence Berkeley Laboratory.

Udell, K.S., and J.S. Fitch (1985), "Heat and Mass Transfer in Capillary Porous Media Considering Evaporation, Condensation and Non-Condensible Effects," 23rd National Heat Transfer Conference, Denver, Co.

van Brakel, J., and P.M. Heertjes (1974), "Analysis of Diffusion in Macroporous Media in Terms of a Porosity, a Tortuosity and a Constrictivity Factor," Int. J. Heat Mass Trans., Vol. 17, pp. 1093-1103.

Wong, R.L., and V.E. Denny (1975), "Diffusion, Flow, and Heterogeneous Reaction of Ternary Mixtures in Porous Catalytic Media," Chem. Eng. Sci., Vol. 30, pp. 709-716.

Wong, R.L., G.L. Hubbard, and V.E. Denny (1976), "Effects of Temperature and Pressure Gradients on Catalyst Effectiveness Factors - I," Chem. Eng. Sci., Vol. 31, pp. 541-548.

7.0 NOMENCLATURE

b	Klinkenberg factor
D_{iK}	Knudsen diffusion coefficient for gas i
D_{12}	effective binary diffusion coefficient (equation 3)
D_{12}^0	binary diffusion coefficient in free space at 1 bar and 0°C.
F	mass flux
g_c	gravitational constant
J	mole flux
J_{iD}	diffusion mole flux
k	permeability
k_B	Boltzmann's constant
K_0	Knudsen diffusion constant
n	molecular density
m	molecular weight
P	pressure
T	temperature
v	mean molecular speed
w	probability factor
x	mole fraction
γ	defined by equation (28)
δ	defined by equation (27)
μ	viscosity
ρ	density
τ	tortuosity
ϕ	porosity
ω	mass fraction

Subscripts

adv	advection
D	diffusion
g	gas
i	species or component
0	base value
1,2	species or component number

Superscripts

ADM	Advective-Dispersive Model
DGM	Dusty-Gas Model

Appendix
Klinkenberg Parameters and Knudsen Diffusion Coefficients

This discussion of the relationship between the Klinkenberg parameter and the Knudsen diffusion coefficients is essentially from Thorstenson and Pollock (1989) except that the temperature dependence has been added.

The Klinkenberg parameter is a function of the porous medium and the gas being used for the measurement. Heid et al. (1950) have correlated the Klinkenberg parameter for air as a function of intrinsic permeability of the porous medium as

$$b_{air} = 0.11 k^{-0.39} \tag{A-1}$$

where b is in Pa and k is the permeability in m^2. The Klinkenberg parameter is proportional to

$$b \propto \mu (T/m)^{1/2} \tag{A-2}$$

so Klinkenberg parameters for other gases can be calculated from

$$b_i = b_{air} \frac{\mu_i}{\mu_{air}} \left(\frac{T_i}{T_{air}}\right)^{1/2} \left(\frac{m_{air}}{m_i}\right)^{1/2} \tag{A-3}$$

where T_{air} is 25°C (298.15 K) if the Heid et al. correlation is used.

Knudsen diffusion coefficients can be calculated from the Klinkenberg parameters as

$$D_{iK} = k b_i / \mu_i \tag{A-4}$$

and the relationship between Knudsen diffusion coefficients for different gases is given by

$$D_{jK} = D_{iK} \left(\frac{m_i}{m_j}\right)^{1/2} . \tag{A-5}$$

The Knudsen diffusion coefficient is also a function of temperature as seen by the dependence of the Klinkenberg parameter, or

$$D_{iK} \propto T^{1/2} . \tag{A-6}$$

Distribution List

Adeyinka E. Adenekan
Exxon Production Research Co.
P.O. Box 2189
Houston, TX 77252

Ronald W. Falta
College of Sciences
Clemson University
P.O. Box 341908
Clemson, SC 29634

Karsten Pruess
Earth Sciences Division
Lawrence Berkeley Laboratory
1 Cyclotron Road
Berkeley, CA 94720

Yvonne Y.W. Tsang
Earth Sciences Division
Lawrence Berkeley Laboratory
1 Cyclotron Road
Berkeley, CA 94720

Geoff A. Freeze
INTERA, Inc.
1650 University Blvd, Suite 300
Albuquerque, NM 87102

Mark Reeves
INTERA, Inc.
6850 Austin Ctr. Blvd, Suite 300
Austin, TX 78731

Mark D. White
Battelle, Pacific Northwest National Laboratory
P.O. Box 999 K9-36
Richland, WA 99352

Kent S. Udell
Department of Mechanical Engineering
University of California
Berkeley, CA 94720

O.A. Plumb
School of Mechanical and Materials
Engineering
Washington State University
Pullman, WA 99164-2920

Thomas A. Buscheck
Lawrence Livermore National Laboratory
P.O. Box 808, L-206
Livermore, CA 94550

John J. Nitao
Lawrence Livermore National Laboratory
P.O. Box 808, L-206
Livermore, CA 94550

George Zyvoloski
Los Alamos National Laboratory
EES-5
MS F665, P.O. Box 1663
Los Alamos, NM 87545

Ron Green
Southwest Research Institute
6220 Culebra Road
San Antonio, TX 78238-5166

Randy Manteufel
Southwest Research Institute
6220 Culebra Road
San Antonio, TX 78238-5166

Internal

MS	Org.
0701 6100	R.W. Lynch
1324 6115	P.B. Davies
1324 6115	S.W. Webb (10)
1324 6115	C.K. Ho
1324 6115	T.L. Christian-Frear
1324 6115	R.J. Glass, Jr.
1324 6115	J. McCord
0750 6118	H.W. Stockman
1328 6749	P. Vaughn
1326 6851	S. Altman
1326 6851	N.D. Francis
1326 6851	J.H. Gauthier
1326 6851	M.L. Wilson
1345 6416	S.H. Conrad
1345 6416	E.K. Webb
1345 6416	P. Kaplan
0719 6621	D.C. Marozas
0719 6621	J. Phelan
0841 9100	P.J. Hommert
0834 9112	M.J. Martinez
0834 9112	R.R. Eaton
0834 9112	C.E. Hickox
0710 6211	G.A. Carlson
1436 1007	C.E. Meyers
9018 8523-2	Central Technical Files
0899 4414	Technical Library (5)
0619 12615	Print Media
0100 7613-2	Document Processing (2) for DOE/OSTI